

Fischer-Tropsch Synthesis to Biofuels (BtL Process)

Reinhard Rauch^{*}, Alain Kiennemann[†], Anca Sauciuc[‡]

^{*}Vienna University of Technology, Institute of Chemical Engineering,
Getreidemarkt 9/166, 1060 Vienna, Austria

[†]University of Strasbourg, LMSPC UMR CNRS 7515, 25 rue Becquerel,
67087 Strasbourg Cedex 2, France

[‡]Department of Renewable Energy Systems and Recycling, Transilvania
University of Brasov, Colina Universitatii 1, 500068 Brasov, Romania

OUTLINE

12.1 Introduction	398	12.5.3 Choice of the Supports	421
12.2 History of FT Synthesis and New Developments in BtL	398	12.5.4 Choice of the Promoters	422
12.3 Syngas: A Renewable Carbon Source from Biomass	403	12.6 FT Reactors	423
12.3.1 Resources and Production	403	12.6.1 Fixed-Bed Multitubular Reactor	423
12.3.2 Syngas Composition: Impurities	409	12.6.2 Fluidized-Bed Reactors	425
12.3.3 Syngas Pretreatment	411	12.6.3 Slurry Reactors	426
12.4 Thermodynamic and Kinetic Considerations of FT Synthesis	414	12.6.4 Microchannel Reactors	427
12.5 Different Kinds of Catalysts	418	12.7 Reaction Conditions at the Laboratory and Industrial Scale	427
12.5.1 Choice of the Metal	418	12.7.1 Operation Conditions	429
12.5.2 Methods of Preparation	419	12.7.2 Aging of the Catalyst	432
		12.8 Mechanism of FT Reactions	435
		12.9 Conclusions	439

12.1 INTRODUCTION

The depletion of fossil fuel reserves, combined with the threat of the anticipated increase in fossil fuel prices and the emissions of greenhouse gases (GHGs) due to the burning of transportation fuel, has led to the development of new, clean technologies to produce biofuels.

Biomass, as a renewable source of energy, has great potential because of the absorption of CO₂ emissions by the growing biomass and the possibility of producing liquid transportation fuels. One of the most known technologies for biofuel synthesis from biomass is the biomass to liquid (BtL) technology. The process consists in the gasification of the biomass, synthesis gas cleaning, Fischer-Tropsch (FT) synthesis, and, finally, hydroprocessing and distillation of the liquid hydrocarbons. The synthetic diesel produced via FT synthesis is environmentally friendly because of the lower concentrations of nitrogen, sulfur, and aromatics. Even though some of the synthetic diesel properties such as density, viscosity, cetane number, and cold flow properties do not fit within the standard limits (EN 590:2004, ASTM D975), by integrating the hydroprocessing stage into the flow of FT synthesis as the final step of upgrading, the synthetic diesel properties can be improved. However, the density of the liquid obtained is too low. A good description of the specifications of different diesel qualities produced by FT synthesis is available [1].

The main objective of this chapter is to evaluate the production of FT diesel using BtL technology. The main issues discussed include the following:

- The history of FT synthesis and the importance of biomass as a new feedstock;
- Gasification of the biomass in order to produce synthetic gas and the pretreatment technologies of the syngas to be able to use it in the FT synthesis;
- FT reactions from the thermodynamic and kinetic points of view;
- Catalysts and reactors used in FT synthesis;
- Specific parameters for the reduction of the catalysts and the operation of the FT reactor;
- Mechanistic consideration of the CO and H₂ chemisorption and activation, surface reaction, and growing chains;
- Deactivation aspects of the catalysts.

12.2 HISTORY OF FT SYNTHESIS AND NEW DEVELOPMENTS IN BtL

Renewable energy sources (RESs) play a significant role in the sustainable energy policies because of their potential for providing energy with low or even zero carbon emissions using solar, wind, geothermal, nuclear, hydrogen, or biomass as energy resources. There is an increasing interest across the world in substituting fossil fuels with renewable energy resources. Using alternative sources of energy can overcome the dependence on fossil fuels, as well as the reserves limitation and uneven distribution implicating economic and geopolitical concerns or GHG emissions. The European Renewable Energy Council expects that, by the end of 2040, the contribution of renewable sources to energy production will increase by almost 50% [2]. In [Figure 12-1](#), the RES scenario by the end of 2040 is presented. As can be seen, biomass is the leader in the total energy consumption (80%)

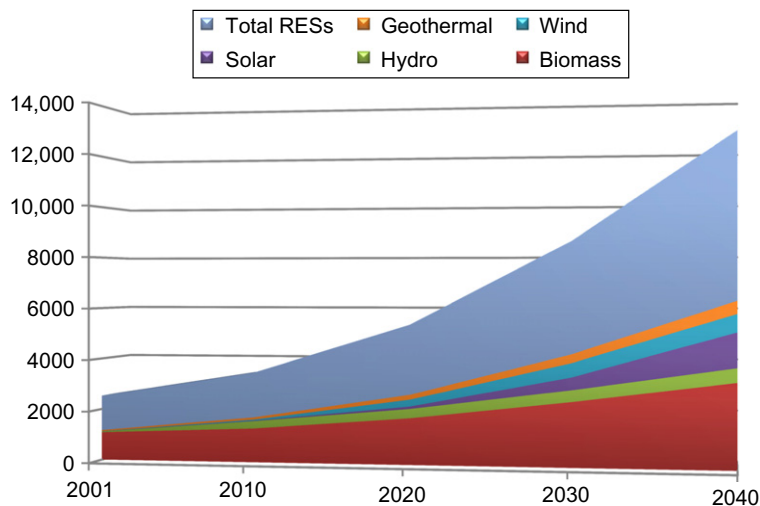


FIGURE 12-1 Renewable energy resources scenario by 2040.

and it is predicted that from 2010 to 2040, the consumption will increase by 60%. Also, based on the 2009/28/EC Directive, by 2020 the contribution of biomass to energy supply should increase by 25% [3].

Thermochemical and biochemical conversion processes of biomass offer the opportunity to transform a valuable resource into energy, biofuels, and biochemicals. Three generations of biofuels can be obtained from biomass conversion: first generation, using vegetable oils, sugar, and starch to produce biodiesel, bioethanol, or biogas; second generation, which converts nonfood crops into FT diesel, bioalcohols, bio-oil, and biohydrogen; and third generation based on algae to produce biodiesel or vegetable oils. Of the three classes, only the first- and second-generation biofuels are developed to the industrial scale. It is predicted that, by 2030, the production of biofuels will increase by 28 times compared with the production in 2000. First- and second-generation biofuels will have the largest contribution in biofuel production [4]. In Figure 12-2, the predicted scenario of global biofuel production by 2030 is presented.

Even though first-generation biofuels rely on well-established technologies, there is continuous criticism related to the competition for food, availability, and efficiency of arable lands, water supply, and production costs. The second generation of biofuels offers the possibility of converting waste or residues and nonfood crop feedstock, leading to a reduction of GHG emissions due to land-use changes to 80-95%, with 40-50% less GHG emissions than the reduction achieved by first-generation fuels [5].

FT and related syntheses transform syngas (hydrogen and carbon monoxide mixture with a ratio near 2) into hydrocarbons and oxygenated compounds into second-generation biofuels. Three main sources of varying importance, namely, natural gas, coal, or biomass, are used in the syngas production step in three integrated processes: i.e., gas to liquid (GtL), coal to liquid (CtL), and biomass to liquid (BtL), respectively.

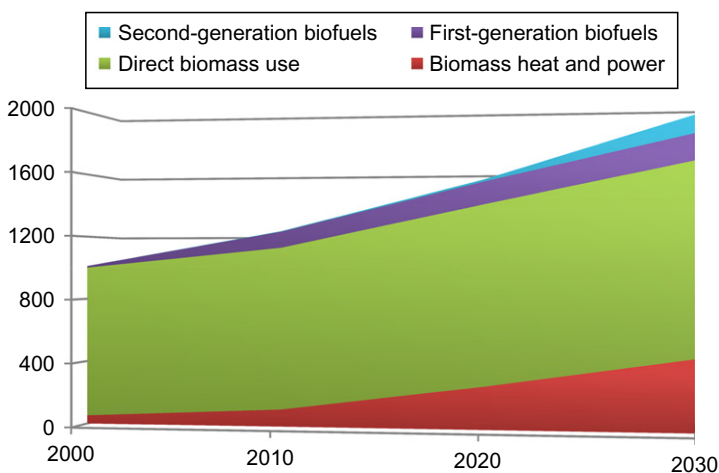


FIGURE 12-2 Global biofuel production by 2030.

The reaction between CO and H₂ on metallic catalysts to obtain methane at atmospheric pressure was discovered in 1902 by Sabatier and Senderens [6]. Methanol synthesis under pressure on zinc oxide-chromium oxide was developed around 1913 by Badische Anilin Soda Fabrick [7]. Finally, in 1923, Fischer and Tropsch published their historic work related to the reaction of synthesis gas on iron doped by alkali [8]. Other catalysts including cobalt and nickel were also tested [9,10]. Research on FT synthetic fuels began in Europe on an industrial scale at the Kaiser Wilhelm Institute in Mülheim and at Ruhrchemie during the 1920s and 1930s, and the first commercial plant was constructed by the end of 1936. Other companies such as Lurgi, Hoechst, and I.G. Farben participated in the development, and 15 commercial plants (9 in Germany, 4 in Japan, and 1 each in France and Manchuria) were operating in the 1940s, but most of them closed during or just after the Second World War. A plant was completed in 1950 at Brownswille (Carthage Hydrocol and Standard Oil, Indiana), but various problems restrained the plant from reaching more than 30% of its design capacity ($360 \times 10^3 \text{ t a}^{-1}$). Despite major modifications, the plant was definitively closed in 1957. This plant was designed to maximize gasoline production based on natural gas as syngas source with an iron catalyst and a fixed fluidized bed operating under pressure and between 305 and 340 °C (high-temperature FT process) (HTFT). The first coal-based SASOL plant (SASOL 1) started in 1955 in South Africa. Compared to the Hydrocol plant, its processing scheme was more complex. SASOL 1 combined both a high-temperature (340 °C) process (HTFT) using a circulating fluidized-bed (CFB) and a low-temperature process (LTFT) (230 °C) using a fixed bed. Both reactors operated under pressure (respectively, 2 and 2.7 MPa), and iron catalysts were used in both processes. The SASOL 1 plant design underwent changes over the years with the improvement of the HTFT process (Synthol process, CFB unit) by SASOL and the use of an LTFT slurry-bed reactor. In 2004, coal gasification was replaced by natural gas reforming, and was shifted from a CtL to a GtL plant.

SASOL 2 started in 1980, and in 1983 SASOL 3 was commissioned (both HTFT plants). Syn-gas was produced from coal using an iron-based FT catalyst. SASOL 2 and 3 were fully integrated and produced gasoline, diesel, and chemicals (160,000 bpd). The initial CFB reactors were replaced in 1993 by SASOL Advanced Synthol reactors. Since 1993, another facility based on a fused iron catalyst and HTFT technology is being operated by Petro SA in Mossel bay, but the plant is supplied with natural gas to produce mainly gasoline (HTFT Synthol technology).

In 1993, in Bintulu Malaysia, Shell started the first facility based on both natural gas and a cobalt FT catalyst. The plant was partly destroyed by an explosion in 1997, but was recommissioned in 2000. Shell developed their LTFT technology based on the Shell Middle Distillate Synthesis (SMDS) process. Heavy paraffins are synthesized in the FT process and then converted to middle distillates by hydroprocessing (14,700 bpd).

The SASOL1 Oryx GTL plant was commissioned in Las Raffan (Qatar) in 2006 using LTFT SASOL technology and a cobalt-based catalyst (SASOL proprietary catalyst). Since 2007, the plant has been producing mainly diesel fuel, and naphtha as a by-product (34,000 bpd). At Las Raffan, the largest GTL plant (Qatar petroleum, Pearl GtL development) was also being constructed (SMDS cobalt fixed-bed technology (140,000 bpd)).

About more or less the same time, new plants were being constructed in Nigeria, and some companies (BP, Amoco, Statoil, etc.) and countries (Iran, Indonesia) are considering plants to produce FT liquid fuels [11,12].

The three primary raw materials for the FT synthesis are coal, methane, and biomass. In the beginning, coal or lignite was the starting material in Germany and South Africa. Actually the opportunity for CtL will be in China and the United States. Methane is the raw material in countries where there is a surplus of natural gas (Malaysia, Qatar, Nigeria, etc.). Both GtL and CtL materials are well adapted to large-scale plants (~100,000 bpd). Small R&D GtL plants are in operation in Italy (ENI, with a capacity of 20 bpd diesel [13]) as well as in Japan, where Nippon GtL Technology Research Association established by JAPEX, JOGMEC, and other corporations completed the construction of a 500-bpd demonstration plant at the Niigata Port industrial park. Nippon GtL Technology Research Association developed a new technology in which the CO₂ contained in natural gas is used in FT synthesis without the need for oxygen supply. Further demonstration tests are currently being conducted in order to develop the technology at the commercial scale.

Multitubular fixed beds were used first in Germany and then in South Africa in the Shell plant. This technology has been chosen for the largest modern plant in Qatar. Fixed-bed reactors (and also slurry reactors) are always associated with the LTFT process with iron- or cobalt-based catalysts. The technology of ebullated beds or fluidized beds is associated with HTFT mainly with iron catalysts. Both LTFT and HTFT have been operated in CtL and GtL plants. The scale is totally different for BtL, which needs to be adapted to the biomass resources and transportation. For BtL, small plants are required that produce some thousands of bpd from local biomass. Depending on the difference of the scales of the different plants, the types of reactors are totally different. Different types of reactor technology have been successively developed depending on the nature of the products required, as well as the operating conditions and the catalysts used, but the exothermicity of the reaction is key to all of their designs.

For BtL, Choren has chosen a multitubular technology, but for smaller plants Velocys is developing a technology with micro and mini reactors [14]. Such technology seems to be particularly well adapted to BtL or to concept GtL on floating production, storage, and offloading vessels.

To produce hydrocarbons from syngas, the catalyst should be able to activate the carbon-oxygen bond, and oxygen atoms need to be removed from the surface by water or CO₂ formation. Breaking of the C—O bond is possible only with a few metals, and only Ni, Co, Fe, and Ru have sufficient activity toward hydrocarbons to be used in commercial applications. Among these four metals, Ru is especially active but its price is around 50,000 times higher than that of iron. Nickel is very active not only for breaking the C—C bond, but also for hydrogenation. So, its selectivity toward methane is very high. Finally, cobalt and iron catalysts are the only two possible candidates. Generally, mainly cobalt is used for waxes and diesel fuel production, and iron for gasoline production. To limit the growing chain, high temperatures (300–340 °C) are used for gasoline production and low temperatures (180–250 °C) for synthesis of waxes.

Figure 12-3 illustrates the fact that, taking into account the nature of the catalysts and the operating conditions (P , T), syngas chemistry (including FT products and oxygenated compounds) is very versatile.

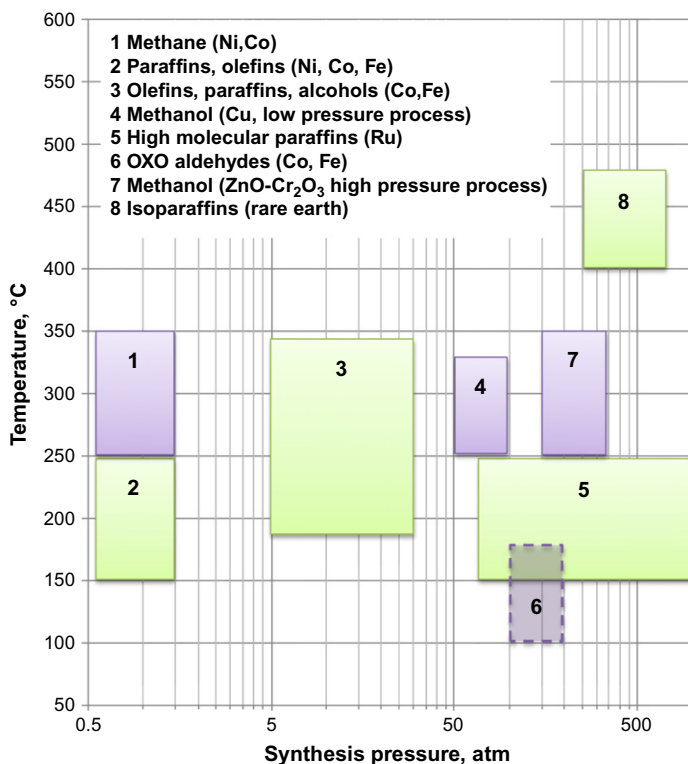
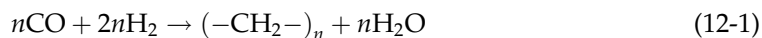


FIGURE 12-3 Pressure-temperature range of reactions of carbon monoxide and hydrogen to give hydrocarbons and oxygenated products.

12.3 SYNGAS: A RENEWABLE CARBON SOURCE FROM BIOMASS

12.3.1 Resources and Production

The FT reaction produces long-chain hydrocarbons from synthetic gas, which is a mixture of H_2 and CO , over Co- or Fe-based catalysts [15–19]. The synthesis can be described as a polymerization reaction, CO being hydrogenated with H_2 to the C_1 intermediate, which then grows to form different hydrocarbons of variable lengths:



In the case of BtL technology, the biomass is converted to synthetic gas by the gasification process, a thermochemical conversion technology operating at 500–1200 °C in the presence of a gasifying agent (air, oxygen, steam, CO_2 , or a mixture of these components) [15]. After the gasification step, the synthetic gas produced contains H_2 , CO , and CO_2 in high concentrations and also small amounts of CH_4 , C_2H_6 , C_3H_8 , aromatic compounds (especially naphthalene, benzene, toluene, and xylenes), tars, sulfur compounds, and nitrogen and chlorine compounds. Because of this, a gas cleaning stage is necessary before using the syngas in FT synthesis. After the FT synthesis itself, the last stage is the upgrading of the FT syncrude in order to obtain high-quality diesel. A schematic view of BtL technology is shown in Figure 12-4 [16].

There are different biomass resources that can be used as gasification feedstock: wood, sawdust, agricultural residues, forest residues, industrial wastes, organic domestic wastes, sludge, etc. [16,20–24]. Analyses of the composition of different types of biomass used as feedstock in the production of synthetic diesel are given in Table 12-1.

As can be seen from Table 12-1, biomass has a low content of sulfur and nitrogen compared to coal, but the heating value of about 18–20 MJ/kg is much lower than that of coal.

For gasification, there are several gasifiers developed at small or large scale. The gasifiers can be classified based on several parameters [15,16,20,25–29] such as the following:

Gasification agent

- air-blown
- oxygen-blown
- steam-blown

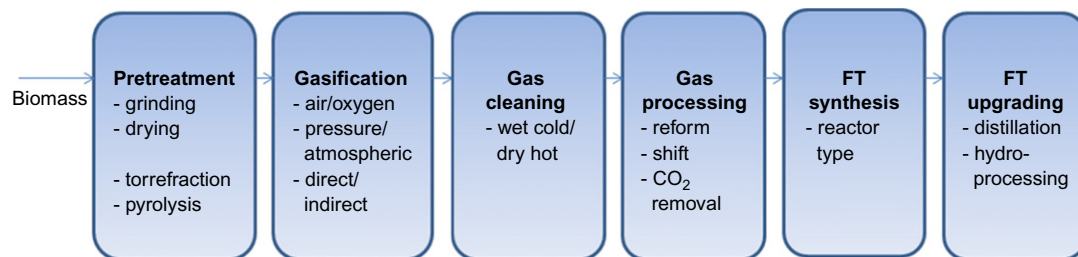


FIGURE 12-4 Schematic view of BtL technology.

TABLE 12-1 Characteristics of Biomass as Feedstock for Synthetic Gas Production

Type	Moisture (wt%)	Heating value (MJ/kg)	Volatile matter (wt%)	Fixed carbon (wt%)	Ash (wt%)	Components (wt%)					Ref.
						C	H	O	N	S	
Black poplar wood	7.1	18.3	86	12.2	1.5	46.1	5.7	47.3	0.8	0.5	[22]
Wood pellet	-	17.1	-	-	0.2	49	6.5	44	0.1	0.05	
Oak acorn	11.9	17.8	75.4	20.6	2.6	41.8	6.8	50.2	0.8	0.2	[22]
Sugar pine	-	-	86.3	13.4	0.3	52.2	6.1	41.1	0.2	0.07	[23]
Radiala Pine	-	-	87.5	12.2	0.3	50.1	6	43	0.2	0.08	[23]
Bark	-	16.2	76	-	7	50.5	6.1	43.2	0.4	0.1	[25]
Pine sawdust	8	20.2	81	18.5	0.5	51.2	5.5	42.2	0.1	0.23	[21]
Grass	6.7	14.6	72	-	38	39.6	5.6	52.7	1.7	0.3	[22]
Maize	11.1	16.4	78.9	19.0	2.1	40.9	6.9	50.7	1.1	0.2	[22]
Wheat	10.3	16.3	80	17.2	2.8	49.2	6.6	47.9	0.2	0.3	[22]
Straw	-	18.2	81.3	-	6.6	49	6	44	0.8	0.2	[25]
Organic domestic waste	54	8.3	-	-	18.9	51.9	6.7	38.7	2.2	0.5	[24]
Sludge	20	9.9	-	-	37.5	52.5	7.2	30.3	7	2.7	[24]
Rape oil	-	35.8	100	-	0	77	12	10.9	0.1	0	[25]
Peat	-	19	74.2	-	2.7	52.6	5.8	40.6	0.4	0.1	[25]
Bituminous coal	-	31.8	34.7	-	8.3	82.4	5.1	10.3	1.4	0.8	[25]

Pressure

- atmospheric gasifiers
- pressurized gasifiers

Temperature

- slagging
- no slagging

Fluid dynamics

- Fixed-bed gasifiers
- Fluidized-bed gasifiers
- Entrained-flow gasifiers

Heat supply

- indirectly heated gasifiers
- directly heated gasifiers

Bed material

- None in fixed-bed or entrained-flow gasifiers
- Catalytic bed material in fluidized-bed gasifiers

Regarding the oxidizing agent used in the gasifier, air has the advantage of being very cheap, but the syngas produced is diluted with a high amount of nitrogen, which increases the downstream equipment size and has a negative influence on FT synthesis with respect to the C_{5+} selectivity. In contrast, when using oxygen as gasification agent, the syngas is not diluted with N_2 , but in this case, oxygen is more expensive and an air separation plant is necessary, which increases the cost of the plant [16]. Steam is easily produced and increases the hydrogen content in the syngas [15], so it can be considered the optimal gasifying agent as it eliminates all the drawbacks of air and oxygen.

In the case of pressure, atmospheric gasifiers have positive aspects of lower cost, and commercial experience with air-blown systems, and indirect gasifiers, while the pressurized gasifiers involve higher costs, smaller volume, biomass feeding problems, high risk in keeping the mass flow constant in the gasifiers, and limited experience. But at the same time, the pressurized downstream system is smaller and more economical at large scales, and increases the heat transfer in the bed, as well as the efficiency of the gas phase reaction and of tar reforming. The main advantage of pressurized gasification is that the syngas produced requires little or no compression [15].

The different types of gasifiers with respect to the fluid dynamics are given in Figure 12-5.

For synthesis gas applications from biomass, mainly fluidized-bed and entrained-flow systems are used. Fixed-bed systems are used only for small-scale air gasification in the area of biomass conversion, as opposed to coal conversion. Four distinct processes occur in the gasifiers as the biomass is converted: drying; pyrolysis, where the tars and volatiles are driven off; reduction; and combustion [27]. The major reactions that take place in combustion and reduction are

- Combustion

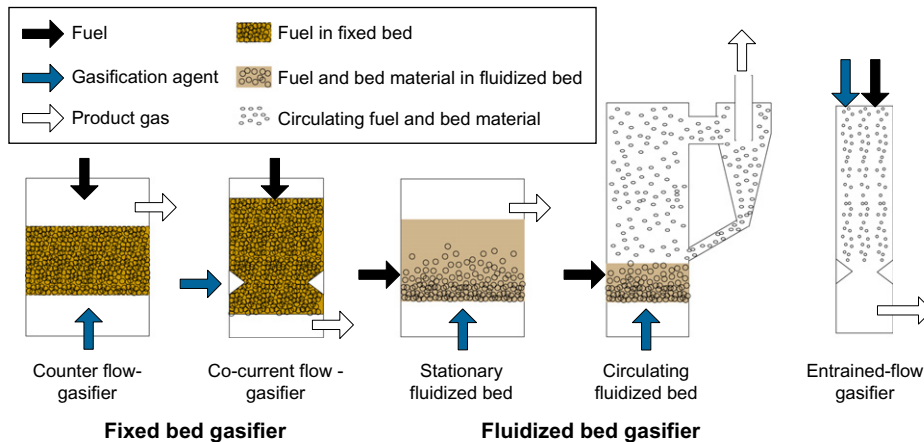


FIGURE 12-5 Principles of gasifiers.

- Gasification



Autothermal gasification (direct gasification) means that the gasification agent oxidizes the fuel inside the gasification reactor directly, providing heat for the process.

Indirect gasification, also named allothermal, employs an external source of energy for the gasification heat. Dual fluidized-bed reactors (DFBRs) are typical examples of indirect gasifiers, where steam is the indirect gasification agent [15]. The concept of the DFBR developed by several researchers [15,16,26] is presented in Figure 12-6.

Many different types of biomass gasifiers have been developed in pilot or demonstration plants in Europe and the United States. In Figure 12-7 and Table 12-2, some projects in Europe are listed that use different types of biomass as feedstock and different types of gasifiers, and the various uses of syngas for biofuel production (FT diesel, methanol, methane, dimethylether (DME)) [20].

In Güssing, Austria, the FICFB (fast internal circulating fluidized bed) process was developed by the Technical University of Vienna and installed in an 8 MW demonstration plant. The combined heat and power (CHP) plant had put in (in 2011) more than 7000 h of operation achieving a maximum total efficiency of 81.3% [30]. A detailed flowsheet of the plant [31] can be seen in Figure 12-8. The plant uses the FICFB system, which produces syngas with a low content of N_2 (below 3 vol%) and a high concentration of H_2 (35-45 vol%). The syngas produced in the FICFB is first cooled down from 850-900 to 150-180 °C and then cleaned in two stages: first, a fabric filter is used to remove the particles, and then, a scrubber (with rapeseed methyl ester (RME) solvent) is used to retain the organic compounds, tars, BTX (benzene, toluene, xylene), naphthalene, inorganic compounds (H_2S , NH_3 , HCN , etc.). After cleaning, the syngas is used either in a gas engine to produce heat and electricity, or in a

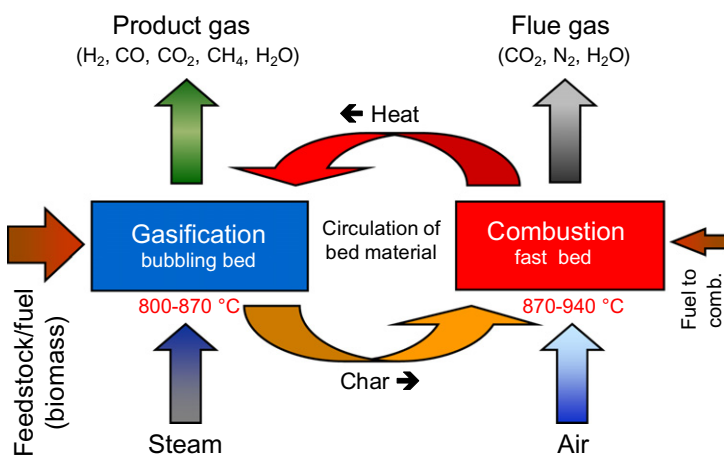


FIGURE 12-6 Principle of steam gasification.

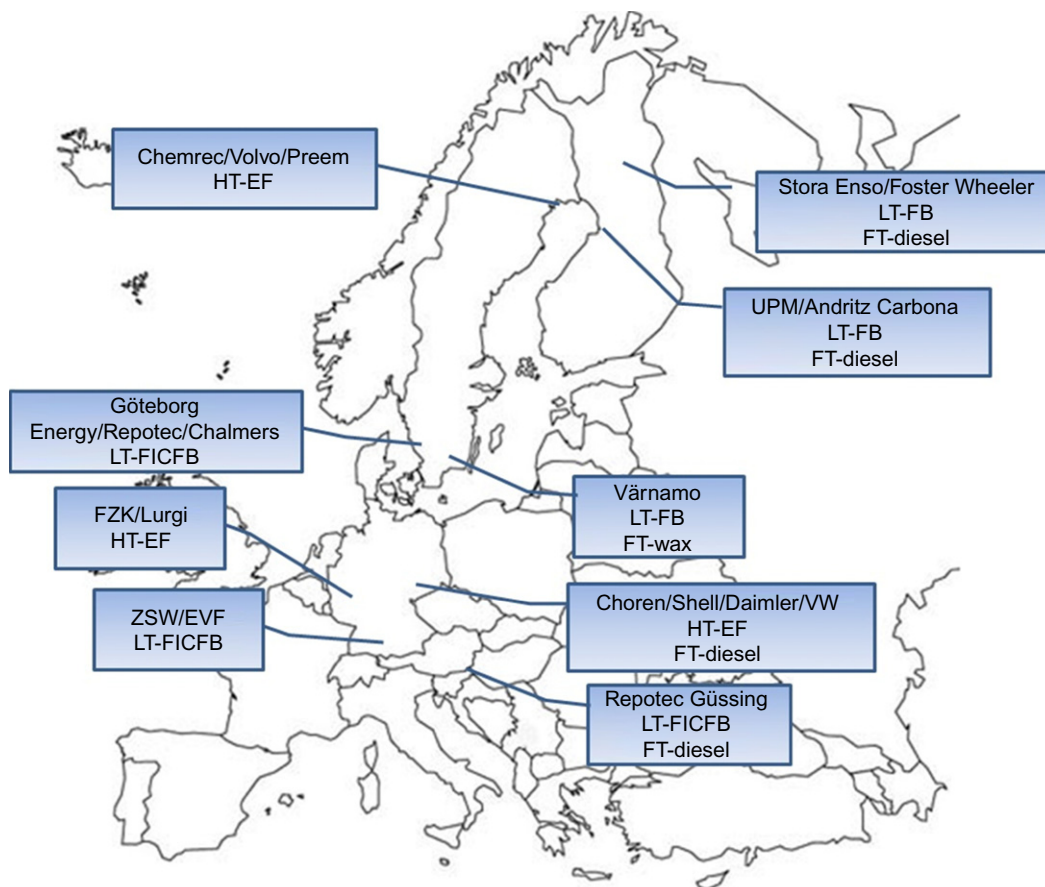


FIGURE 12-7 Biomass gasification plants for biofuel production.

laboratory FT plant and a demonstration BioSNG plant. The flue gas is cooled, cleaned of ash, and released into the atmosphere via a chimney.

In Germany, three projects are in development for forest and farm residue gasification:

- The Institute ZSW in collaboration with Baden-Württemberg local utility (EVF) is developing an LT-FICFB system to produce BioSNG.
- Karlsruhe Institute (FZK), together with Lurgi, is promoting the high-temperature entrained-flow technology for gasification of biomass with oxygen under high pressure and temperature.
- A similar technology was also developed by Choren Company, together with Daimler, VW, and Shell (Carbo-V technology), to produce FT diesel.

In Sweden, an FICFB system is planned by Goteborg Energy in alliance with Repotec and MetsoPower to demonstrate the first semicommercial 20 MW BioSNG plant [20]. Another

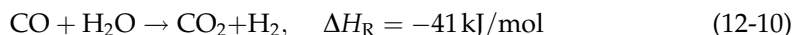
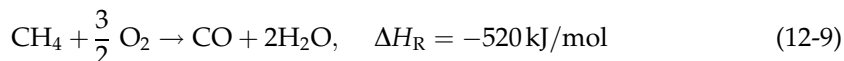
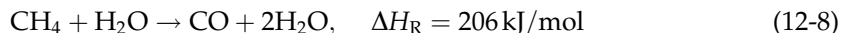
demonstration plant was built in Värnamo, with pressurized CFB gasification technology. Chemrec has developed entrained-flow technology for black liquor gasification to produce DME or methanol.

Two other projects are running in Finland: first, a collaboration between VTT, Neste Oil, and Stora Enso (pulp and paper industry), and another between UPM and Andritz/Carbona. Both projects have integrated a fluidized-bed gasifier system to transform forest residues into FT liquids [20].

Other small projects promoting biomass gasification technologies include the Milena gasifier from ECN, The Netherlands, and in Vermont, USA [15], the Institute of Gas Technology, and Batelle Columbus Laboratory, USA [12,25,29]. In Table 12-3 are summarized all the projects discussed, with their characteristic parameters for gasification.

12.3.2 Syngas Composition: Impurities

As was shown earlier, the composition of the syngas depends on the gasification technology adopted, the oxidizing agent, and the feedstock. There is an important difference between the syngas composition obtained from biomass and that from natural gas. A GtL plant includes the conversion of natural gas to synthesis gas through steam reforming, dry reforming, partial oxidation (POX), or oxidative steam reforming (autothermal reforming (ATR)) [35]. POX produces syngas with an H_2/CO ratio less than 2 with little CO_2 , CH_4 , and N_2 , while for ATR, the H_2/CO ratio is higher (>2) with, however, more CO_2 and CH_4 . The given nominal syngas composition could be modified to satisfy the FT requirements by changing the pressure, temperature, and percent of CO_2 present [36]. ATR is one of the most suitable processes for natural conversion to syngas with an H_2/CO ratio of almost 2, which is necessary in the FT synthesis. In ATR, the main reactions are methane reforming with steam, POX, and water-gas shift (WGS) reaction [35,37]:



In the case of biomass gasification, the composition of the synthesis gas produced can vary over a wide range, with H_2/CO values between 0.45 and 2, or even higher, due to the WGS reaction. It was shown that syngas derived from biomass has a lower H_2/CO ratio than that obtained from natural gas and that it contains contaminants— H_2S , COS , NH_3 , tars, dust, and alkali [19]. The H_2/CO ratio depends on the following:

- type of gasification agent used and gasification agent/biomass ratio—the higher the steam/biomass ratio, the higher the steam partial pressure, increase of WGS reaction, and shift toward H_2 production. Thus the H_2/CO ratio is increased [15];
- temperature of gasification—a higher temperature means more endothermic gasification reactions and thus the increase of the concentration of H_2 and CO [15];
- principle of gasifier—pressurized or atmospheric, direct or indirect heated, fluidised bed or entrained flow

TABLE 12-3 Characteristics Parameters of Biomass Gasification Projects Developed Across the World

	Repotec Güssing	Choren Freiberg [32]	Cutec [33]	Goteborg Energy	Vermont	Milena		MIUN	IGT	BCL	Westinghouse [34]
Technology	BFB	Carbo-V EF	CFB	BFB	CFB	CFB	CFB	BFB	Direct, oxygen- blown	Indirect, air- blown	Plasma PGVR
Bed material	Olivine	-	-	Sand	Sand	Sand	Sand	Sand	-	-	-
Feedstock	Biomass chips	Wood chips	Chips	Wood pellets	-	Wood chips	Wood pellets	Wood pellets	Poplar wood	Poplar wood	
Gasification temperature (°C)	900	1200 1500	950	812		850	850	800	982	863	1500-5500
Pressure (bar)	atm.	5	atm.	atm.	atm.	atm.	atm.	atm.	34	atm.	atm.
Composition (%)											
H ₂	35-45	37.2	31.6	25.1	15	21.4	18-20	46	20.8	16.7	15.8
CO	20-30	36.4	22	33.1	50	39.3	37-39	35	15	37.1	40
CO ₂	15-25	18.9	33.6	14.8	10	13.9	11-13	10	23.9	8.9	3.5
CH ₄	8-12	0.06	-	11.8	15	12.8	14	11	8.2	12.6	-
N ₂	1-3	0.1	3	9.3	-	-	-	4	0.4	0	-
Tar content (g/m ³)	1.5-4.5	-	9.5	7.8	-	32	40	10-46	-	-	-

- type of catalyst used in FT synthesis—an Fe-based catalyst has higher WGS activity than a Co-based catalyst and increases the H₂/CO ratio [19].

The influence of syngas composition in the FT reaction was investigated by several researchers [19,38–40], and the following observations were made:

- H₂/CO ratio has a significant impact on CO conversion, C₅₊ selectivity, product distribution, and chain growth probability;
- a low inlet H₂/CO ratio leads to selectivity to longer hydrocarbons (increase of C₅₊ selectivity) and a drop in the hydrocarbon formation rate due to the decrease in productivity of the catalyst;
- reduction of the hydrogen in the feed leads to a lower selectivity to CH₄, but an increase in the olefin/paraffin ratio;
- CO conversion increases at high H₂/CO.

12.3.3 Syngas Pretreatment

As was shown earlier, the synthesis gas produced from biomass contains several undesirable components such as NH₃, HCN, H₂S, COS, HCl, particulates, and tars. In Table 12-4, the impurities of the syngas and their specific cleaning stages to achieve the requirements for FT synthesis are listed [15,16]. As can be seen, there are two ways to clean the synthesis gas:

- wet cold gas cleaning, which is the conventional method;
- dry hot gas cleaning.

Wet cold gas cleaning or conventional gas cleaning has been proven and applied successfully in industrial FT installations. The main disadvantages are the production of liquid waste sludge (difficult to dispose) and the loss of thermal efficiency due to the reduction of temperature at near ambient conditions [15,28,41]. Conventionally, the technology consists in syngas cooling, low-temperature filtration, and scrubbing with different solvents at temperatures between –50 and +100 °C [29]. The flowsheet of wet cold gas cleaning is presented in Figure 12-9. The first step in syngas cleaning is tar removal. Tars represent all the organic compounds with medium to high molecular weight condensing under ambient conditions [15,29]. There are undesirable components that block the filters and valves, initiate metallic corrosion, and deactivate the FT catalyst. Therefore, their complete removal is required (Table 12-4). The concentrations of tars can be reduced in wet cold gas cleaning starting inside the gasifier, by using high-temperature operation, increasing the residence time of the gas, and adding catalytic materials with high activity for cracking (dolomite, olivine, iron ore, or nickel- or ruthenium-based catalysts). Another step in tar removal is the cyclone separation of the solids and aerosol from the gas. The main drawback of this step is the agglomeration of tars with particulates, which deposit on the cyclone surface [15]. After the separation of tars and particulates, the gas has to be cooled down before using a bag filter for the removal of particulates and alkali. Inorganic sulfur, nitrogen, and chlorine compounds are removed with scrubbers and different solvents (NaOH, H₂SO₄, Rectisol, Selexol, methyldiethanolamine). Finally, because the FT catalyst, especially Co-based, is very sensitive to sulfur compounds,

TABLE 12-4 Gas Cleaning Stages for Syngas Contaminants [15,16]

Contaminant	Poplar wood (%)	FT cleaning requirements (ppb)	Cleaning efficiency required (%)	Cleaning step	
				Wet cold	Dry hot
Particulate	1.33	0	>99.9	- Cyclone - Bag filter - Scrubber	- Granular bed - Metallic filter - Ceramic candle filter - Cyclone
HCN+NH ₃	0.47	20	>99.9	- Scrubber (H ₂ SO ₄) - Chemical and physical acid removal (Rectisol, Selexol, MDEA)	- ZnO, CuO guard bed
H ₂ S+ COS	0.01	10	>99.9	- Scrubber - ZnO, CuO guard bed - Activated charcoal - COS hydrolyzation	- Safeguard filter - ZnO, CuO guard bed - Sorption bed of α -Fe
Alkali	0.1	10	>99.9	- Condensation on particulates by cooling down	- Adsorption and chemisorption
HCl	0.1	10	>99.9	- Absorption by dolomite (in tar cracking) - Bag filter (reaction with particulates) - Scrubber (NaOH)	- Dry fly ash
Tars	-	0	>99.9	- Scrubber (organic oil—RME)	- Catalytic, thermal reforming

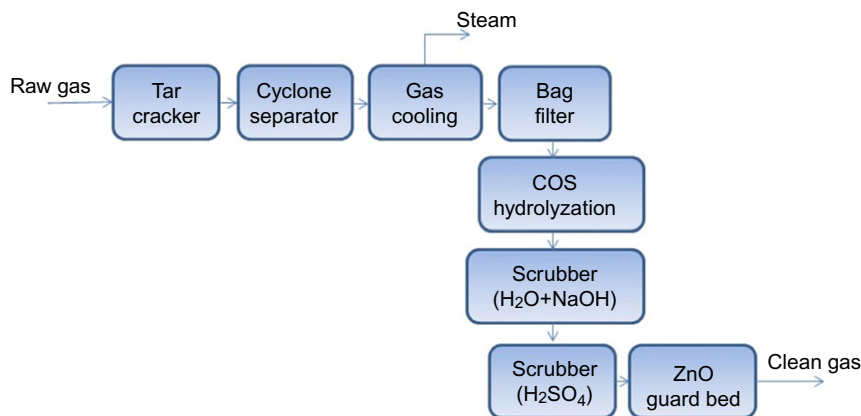


FIGURE 12-9 Wet cold gas cleaning scheme.

catalytic guard beds (ZnO, CuO, and activated char) are used to get the concentration of contaminants below 10 ppb.

A wet cold gas cleaning technology is applied in the FT pilot plant in Güssing (Figure 12-10), which operates with a slurry reactor (volume 20 l) and a Co-based catalyst at the following operating conditions: temperature 230 °C; pressure 20 bar; and gas flow 5 Nm³/h [30,31]. The synthesis gas received from the CHP plant is dried and cleaned of naphthalene and BTX with an RME scrubber. Sulfur components are removed below 5 ppb with an activated charcoal reactor at ambient temperature and pressurized fixed-bed reactors with ZnO and CuO adsorbers at a temperature between 70 and 250 °C and pressure 15-25 bar.

Dry hot gas cleaning (Figure 12-11) can be a more efficient technology because of the advantages on the overall energy balance (when using a reformer or shift reactor that requires high inlet temperature) and lower operation costs [29]. However, if the gasifier is operating at lower pressure, the benefits of hot gas cleaning are less because the syngas has to be cooled for compression to FT pressure. Other disadvantages are that dry hot cleaning has not been commercially applied yet, being still in the experimental phase. There is also uncertainty regarding the achievement of the standard purification requirements for FT synthesis [20]. In the case of tars, the dry hot steps are efficient:

- thermal and catalytic reforming inside the gasifiers using a temperature around 1000-1300 °C and catalytic bed materials [41];
- monolith reactors—ceramic blocks with active materials (Ni-based catalyst) on a honeycomb structure [15];
- catalytic filters—with an integrated fixed bed of Ni-based catalyst grains for tar cracking as well as particulate separation [15,28].

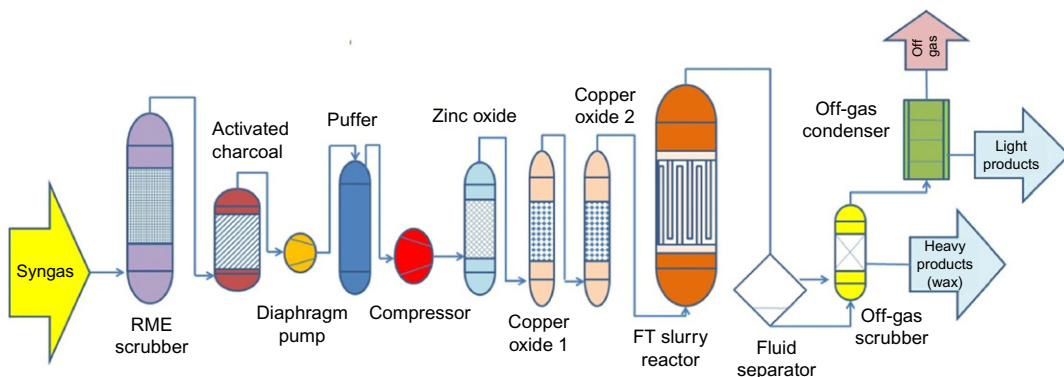


FIGURE 12-10 Flowsheet of the Fischer-Tropsch plant, Güssing, Austria.

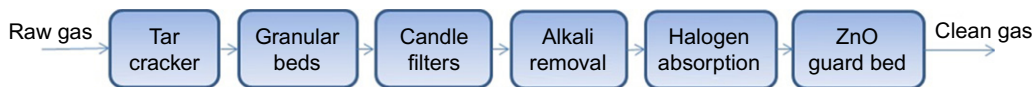
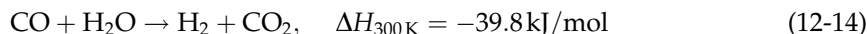
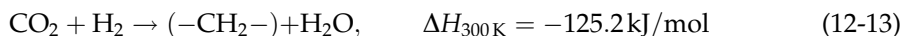
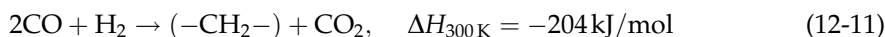


FIGURE 12-11 Dry hot gas cleaning process.

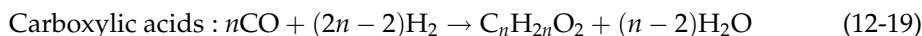
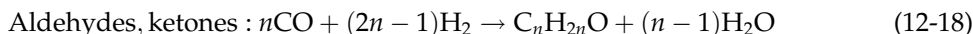
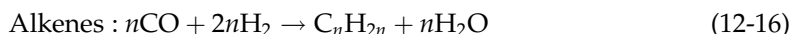
Alkali can be removed by adsorption or chemisorption at 750-900 °C, but there are some components such as lead or zinc that cannot be removed at these temperatures [29]. Also, in the case of halogen, sulfur, and nitrogen components, the existing dry hot cleaning steps may not be enough for the required removal. Further research has to be conducted to improve the high-temperature cleaning technologies.

12.4 THERMODYNAMIC AND KINETIC CONSIDERATIONS OF FT SYNTHESIS

FT synthesis produces both saturated and unsaturated hydrocarbons based on Equation 12-1, which is a highly exothermic polymerization reaction with a negative enthalpy $\Delta H_{300\text{K}}$ of 165 kJ/mol [35,42,43]. Other possible reactions [35] include

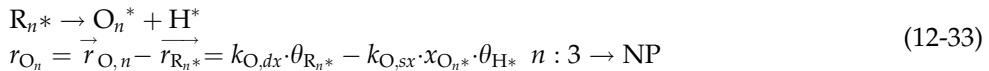
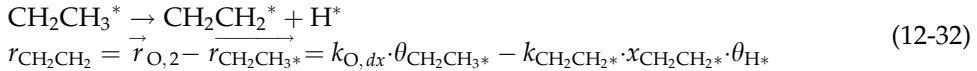
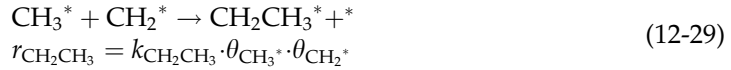


The desired products (paraffin, olefin, alcohols) as well as undesired ones (aldehydes, ketones, esters, acids, carbon) can be formed during FT synthesis [42,44,45]:



As can be seen, the main FT reactions are highly exothermic and hence the necessity for cooling the FT reactor to secure stable reaction conditions [35]. A more detailed FTS reaction mechanism (with the related kinetic rate equation) to describe the CO dissociation and the addition of H₂ and C involves the carbide theory (for CO conversion) and alkyl mechanism (for chain growth process), where * represents an active site [17,18,46,47]:





where p_{H_2} , p_{CO} are the partial pressures of H_2 and CO , θ is the fraction of free catalytic sites, θ_i is the fraction of the catalytic sites occupied by species i , R_n is the generic linear-growing adsorbed hydrocarbon species, P_n is the generic linear paraffin, O_n is the generic linear α -olefin, x_{O_n} is the molar fraction of the α -olefin n in the liquid phase surrounding the catalyst pellets, k_i is the kinetic constant of step i , and NP is the highest carbon number that can be found in the products.

The mechanism involves H_2 adsorption on two catalytic sites in the dissociated state (Equation 12-20), CO adsorption in the molecular state (Equation 12-21), dissociation (Equation 12-22), and subsequent addition of H^* to form methylene species and water (Equations 12-23–12-26). Based on the alkyl mechanism, the chains' initiation and growth start with the formation of methyl species (Equation 12-27) and subsequent insertion of CH_2^* in the active site—alkyl species (Equations 12-28–12-30). Methane is considered to be formed from a methyl species and a surface hydrogen atom (Equation 12-28). Termination of the chain groups occurs by the interaction between the intermediate R_n and a surface hydrogen

atom to form paraffin (Equation 12-31) or by β -hydride elimination of an H^* species to form α -olefin (Equations 12-32 and 12-33). For each step, elementary rates have been assigned and for the first two steps, process conditions have been determined, while the other steps are assumed to be nonreversible and kinetically controlled [17,18]. The kinetic constant k_i can be described by the Arrhenius law [17,46]:

$$k_i = k_i^0 \exp\left(-\frac{E_i}{RT}\right) \quad (12-34)$$

where k_i^0 is the pre-exponential factor of each step, and E_i is the activation energy.

Based on the effect of partial pressure of reactants, several other kinetic models for describing the FT rate of reaction have been proposed and reviewed by several researchers [37,48–50]. In Table 12-5, different kinetic models of the FT synthesis found in the literature are summarized.

The kinetic expressions described for the FT synthesis are in direct correlation with the catalysts used: Co- or Fe-based catalysts. The constants a , b , and \hat{a} are different and have to be found for each catalyst. In case of an Fe-based catalyst, the partial pressures

TABLE 12-5 Summary of the FT Synthesis Kinetic Models

Model	Catalyst	Kinetic expression
Brotz [48,50]	Co/MgO/ThO ₂ /kieselguhr	$r_{FT} = \frac{ap_{H_2}^2}{p_{CO}}$
Yates and Satterfield [35]	Co/Al ₂ O ₃	$r_{FT} = \frac{ap_{H_2}p_{CO}}{(1 + bp_{CO})^2}$
Anderson [48–50]	Co/ThO ₂ /kieselguhr	$r_{FT} = \frac{ap_{H_2}^2p_{CO}}{1 + bp_{CO}p_{H_2}^2}$
Yang [48]	Co/CuO/Al ₂ O ₃	$r_{FT} = ap_{H_2}p_{CO}^{-0.5}$
Pannell [50]	Co/La ₂ O ₃ /Al ₂ O ₃	$r_{FT} = ap_{H_2}^{0.55}p_{CO}^{-0.33}$
Wang [50]	Co/Al ₂ O ₃	$r_{FT} = ap_{H_2}^{0.68}p_{CO}^{-0.5}$
Rautavuoma and van der Bann [51]	Co/Al ₂ O ₃	$r_{FT} = \frac{ap_{H_2}p_{CO}^{0.5}}{(1 + bp_{CO}^{0.5})^2}$
Sarup and Wojchichowsky [48–50]	Co/kieselguhr	$r_{FT} = \frac{ap_{H_2}^{0.5}p_{CO}}{(1 + bp_{CO} + cp_{H_2}^{0.5})^2}$ $r_{FT} = \frac{ap_{H_2}^{0.5}p_{CO}^{0.5}}{(1 + bp_{CO}^{0.5} + cp_{H_2}^{0.5})^2}$
Prins [37]	Co/Al ₂ O ₃	$r_{FT} = \frac{ap_{H_2}p_{CO}}{(1 - bp_{CO})^2}$
Ledakowicz [1]	Fe-based catalyst	$r_{FT} = \frac{p_{H_2}p_{CO}}{p_{CO} + \hat{a}p_{H_2O} + bp_{CO_2}}$

for water and CO₂ have to be taken into consideration because of the high WGS reaction activity [48].

In terms of the product distribution of FT synthesis, the Anderson-Schulz-Flory (ASF) model is described as a chain polymerization kinetic model with the addition of one carbon on the chain, based on a constant chain growth probability [18,35,37,52,53]:

$$M_n = (1 - \alpha)\alpha^{n-1} \quad (12-35)$$

where M_n is the mole fraction of the product with carbon number n , and α is the chain growth probability.

With the logarithmic form of Equation 12-37, it is possible to plot the product mole fraction and to calculate the α value from the slope of the plot.

$$\ln M_n = n \ln \alpha + \ln \left(\frac{1 - \alpha}{\alpha} \right) \quad (12-36)$$

According to this equation, the plot of $\ln M_n$ versus the carbon number n should give a straight line [54]. But in practice, deviation from the “ideal” ASF model has always been observed. An example of the product distribution with two distinct slopes can be seen in Figure 12-12 [55]. Based on these observations, a modified ASF model has been proposed that uses two chain growth probabilities for the total product distribution [52–55]:

$$M_n = A\alpha_1^{n-1} + B\alpha_2^{n-1} \quad (12-37)$$

$$\ln M_n = \ln [A\alpha_1^{n-1} + B\alpha_2^{n-1}] \quad (12-38)$$

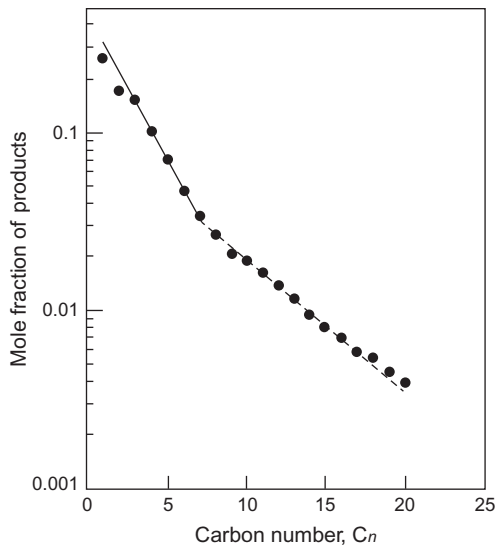


FIGURE 12-12 ASF plot for a potassium-promoted iron catalyst.

At the break point of the ASF diagram, the contributions of the two terms from Equation 12-39 are equal:

$$A\alpha_1^{n-1} = B\alpha_2^{n-1} \quad (12-39)$$

where $n = \zeta$, and ζ is the break point.

Therefore, we have

$$B = A \left(\frac{\alpha_1}{\alpha_2} \right)^{n-1} \quad (12-40)$$

The sum of the mole fraction is unity:

$$\sum_{n=1}^{\infty} M_n = \sum_{n=1}^{\infty} [A\alpha_1^{n-1} + B\alpha_2^{n-1}] = 1 \quad (12-41)$$

As was demonstrated, methane and ethane do not obey the ASF model. It seems that the quantity of methane is more than that predicted, especially on the Co-based catalyst, which favors the methanation reaction. In case of ethane and even propane, there is much less concentration than predicted, due to the secondary reaction of olefins to incorporate into the polymer by initiating a new chain [54]. Because of this, C_1 and C_2 can be removed from the ASF equation, leading to Equation 42:

$$\sum_{n=1}^{\infty} M_n = \sum_{n=1}^{\infty} [A\alpha_1^{n-1} + B\alpha_2^{n-1}] - A(1 + \alpha_1) - B(1 + \alpha_2) = 1 - M_1^{\text{exp}} - M_2^{\text{exp}} \quad (12-42)$$

Different authors have reported deviations from the ASF model even outside the C_1 - C_5 product range [54]. These deviations can be explained by

- the impossibility to maintain the parameters and conditions of the FT synthesis: namely, temperature, H_2/CO ratio, pressure, and partial pressure of the reactants;
- the secondary reactions on the catalyst surface, especially in the case of olefins;
- the evaporation of light FT products during the reaction and the difficulty in their condensation;
- the errors due to the quantitative analysis of the products.

12.5 DIFFERENT KINDS OF CATALYSTS

12.5.1 Choice of the Metal

The products of an FT synthesis could be varied to some extent by the conditions of the reaction or by the system carrying out the reaction. However, the real key to obtaining good selectivity toward a given family of products and activity is the catalyst composition. All elements of group VIII (in metallic form) that are able to chemisorb CO dissociatively (into C and O) and H_2 have a noticeable activity [56], but only four (Ru, Co, Fe, and Ni) have sufficient activity for commercial application [11,57]. In fact, only two (Co, Fe) are of industrial interest for FT synthesis as main metals in the catalyst formulation. Early works on unsupported metals gave the following specific activity: $Fe > Co > Ni > Rh > Ru$ [58]. However, it has been demonstrated that activity changes with the nature of the support: $Ru > Fe > Ni > Co > Rh$ on

alumina [59] and $\text{Co} > \text{Fe} > \text{Ru} > \text{Ni} > \text{Rh}$ on silica [60]. Even though ruthenium is one of the most active, at least on alumina, its price (about, respectively, 50,000 and 500 times more expensive than iron and cobalt) and scarcity limit its use as promoters [11]. Nickel is also very active, but its hydrogenation power is too high compared to its growing chain power and it leads to the undesired formation of large amounts of methane together with low olefin formation [61]. Selectivity to methane decreases following the sequence $\text{Ni} > \text{Rh} > \text{Co} > \text{Fe}$ [62], while olefin selectivity is the most important for iron catalysts ($\text{Fe} > \text{Co} > \text{Ni}$) [62]. Iron catalysts also oxygenate compounds as by-products (alcohols, ketones), which is a consequence of the presence of stable Fe_3O_4 (magnetite) during the synthesis.

Taking into account the classification of activity on unsupported metals [58], iron catalysts were initially tried but then abandoned because of the low liquid hydrocarbon yields and short catalyst life. However, after the discovery that use of pressure (15 atm.) increased the catalyst life by several times and doubled its yield [63], iron catalysts have begun to receive a great deal of attention particularly in Germany and then in South Africa. From one formulation to another, the ratio between iron and other elements changes, but most of the iron catalysts contain copper, potassium oxide, and silica, specifically referring to Ruhrchemie patents. A typical composition is the following: 100 Fe, 5 Cu, 5 K_2O , 23 SiO_2 [63–65]. Much information on iron catalysts can be found in reviews [66,67]. For the production of gasoline and α -olefins, iron catalysts are the best option when operating at high temperatures of about 350 °C (HTFT). For the production of diesel fuel or waxes (220 °C, LTFT process) with very little alcohol and methane formation, cobalt catalysts are more active than their iron counterparts (2–3 times). In the first formulations, cobalt was deposited on kieselguhr or bentonite, and catalysts promoted by thorium or magnesium oxides [68,69]. The technology with cobalt catalysts has been developed mainly in the last 30 years and now cobalt catalysts present high stability, high conversion per pass, good aging, and high productivity. Cobalt certainly represents the optimal choice for long-chain hydrocarbon synthesis in the LTFT process [70].

Differences other than the optimal temperature of operations exist between Co and Fe catalysts. The required H_2/CO ratio (about 2 for Co; 0.5–2.5 for Fe) could be an advantage for iron if gases coming from biomass or coal gasification are used [57,70]. The WGS reaction is significant with iron catalysts, but the operation conditions need to satisfy both FT and WGS requirements. With cobalt, the H_2/CO ratio has to be controlled externally by a separate reactor. From a mechanistic point of view, it is generally admitted that the O coming from CO dissociation is eliminated on Co as water by reaction with hydrogen, while with iron it is eliminated as CO_2 by reaction with carbon monoxide. This explains the difference in the optimal H_2/CO ratio between the two metals. As soon as surface carbon is formed, it can react with both iron and cobalt to form carbides, but Fe carbides are more stable. Finally, catalysts are poisoned by sulfur compounds (H_2S or COS), but deactivation of iron is more severe than that of cobalt [67].

12.5.2 Methods of Preparation

The methods of preparation will directly impact the structure, texture, or morphology of the catalyst. The final goals are as follows:

- obtaining the appropriate dispersion of the catalysts (size of metal particles),
- controlling the porosity of the support,
- favoring or disfavoring interactions between metal particles and the supports and/or promoters.

The methods of preparation could also strongly influence the diffusion effects and the aging of the catalysts.

Numerous methods of preparation have been described in the literature. Incipient wet impregnation (capillary impregnation) of a support by a solution of metal salts, where the specific area and porosity of the support are well known, is the most common method. The solution of metal salt (often a nitrate dissolved in water) is contacted with a dry porous support. All pores of the support are filled, and the amount of solution is calculated to just fill the porous volume of the support. This impregnation can be done with or without the interaction between the metal precursor and support. The main point is the control of the pH of the salt solution in accordance with the point of zero charge (PZC) of the support. Temperature and concentration of the salt solution also play a role. Alumina, silica, or titania are commonly used as support, but too high or too low pH can partly dissolve SiO_2 and Al_2O_3 , respectively, and favor the formation of defined structures (silicalite, spinel) between the metallic oxide and the support. It may be noted that SiO_2 , Al_2O_3 , and TiO_2 supports have been developed, respectively, by Shell, Sasol and Statoil, and Exxon [71]. As an example, in the case of cobalt, for which impregnation is very common including with industrial catalysts, if the pH is lower than 2 (the PZC of SiO_2), the surface of silica will be positively charged and the Co^{2+} ions poorly dispersed. In the range $2 \leq \text{pH} \leq 5$, adsorption of Co^{2+} ions is favored on the negatively charged surface and the dispersion improves. If the $\text{pH} > 5$, Co^{2+} ions react with silica to form cobalt silicate, which is inactive in FT synthesis [72]. A wet impregnation (large excess of liquid compared to the pore volume) forming a slurry, with slow evaporation of the excess liquid at moderate temperature and under stirring, is also used [73].

Coprecipitation has been better developed for iron than for cobalt for the metallic precursor alone or for supports such as Mn-Al, Zn-Al, or Zr oxides [74]. Coprecipitation is obtained when the solubility of the salt precursors is abruptly modified by the addition of an alkali carbonate (Na, K), hydroxide (Na, K), or ammonia (pH change). However, to coprecipitate two or more components at the same time, the products of the solubility of all the components need to be similar. The nature of the precipitating agent, the starting metallic salt, the addition conditions, and the temperature and time of precipitation [75] are the main parameters for controlling the size of the precursors of metallic particles and for the formation of defined compounds between metallic oxides and support. Because of these constraints, precipitation is largely developed for iron but less for cobalt catalysts.

The sol-gel method has been developed to prepare metal/ SiO_2 catalysts with tetraethoxysilane as the SiO_2 precursor. Pore size modifiers such as polyalcohols are often used. The final goal is the formation of a uniform distribution of metal particles (generally of a smaller size than with other methods) as well as the control of porosity and surface area [76,77]. The main drawbacks lie in the difficulties to reduce the metal precursor due to the possible occlusion of the metal into the silica and metal silicalite formation as well as the high cost and the scale-up of the preparation. Finally, other preparation methods such as colloids and microemulsions have been described in detail in the literature [70].

For all the methods, and more specifically for cobalt catalysts, an optimal size of cobalt particles is needed. The effect of the metal particle size has been amply demonstrated. Iglesia *et al.* [78–80] showed that, for large cobalt metal particles, the reaction rate is proportional to the number of cobalt surface sites (cobalt/alumina, silica, titania supported catalysts), and Bezemer *et al.* [81] proved that the turnover frequency was almost independent of cobalt

particle sizes larger than 6-8 nm. For this range of particle size, the FT reaction corresponds to a structure-insensitive reaction. It has been demonstrated by thermodynamic calculations that metal particles smaller than 4 nm could be reoxidized by water during the reaction. Reoxidation of particles in real FT conditions is under debate and will be discussed later in relation to the aging of the catalyst.

All these methods of preparation give, after calcinations and reduction, metal particles that are well distributed at the surface of the grains. However, due to the exothermicity of the reaction, studies have been devoted to the control of the metal concentration profile and to avoid mass-transport restrictions. This is the reason why eggshell catalysts have been evaluated for FT fixed-bed reactors [82]. The preparation of eggshells is based on the impregnation method, but requires a careful control of the properties of the solution of the starting salt (competitive impregnation, use of solvent with high viscosity, or chelated metal complexes) [82–84]. To overcome the pressure drop and diffusion limitations, a monolith (cordierite, γ - Al_2O_3 , steel, SiC) impregnated by the metal precursor salt can be a solution [85,86].

After the preparations discussed earlier, a catalytic precursor is formed. A step including decomposition of the precursor into a metallic oxide phase followed by a reduction into metal is absolutely essential to have an active catalyst. Reduction depends on numerous parameters. Among them are the nature of the starting metallic salt, the thermal pretreatment, the reducing gases (H_2 , CO, syngas), the percentage of metal added, the support, and the promoters. If reduction occurs with hydrogen, the dilution, flow, and the pressure of hydrogen can change the percentage of the final reducibility.

12.5.3 Choice of the Supports

Supports not only play a role in the dispersion of metallic precursors but also act as a binder or a spacer and induce interactions between the oxide precursors and supports. This exerts an effect on the activity, selectivity, and aging. The most common carriers are silica, alumina, and titania, but recently, carbon and silicon carbide structures have been developed. Interactions between metal precursor and support are of prime importance to achieve a good dispersion of the active particles and to modify the reducibility of the metallic oxide. Too strong metal-support interaction should be avoided, as it will decrease the percentage of reduced metal and, consequently, the catalytic performance. Too weak support interaction involves the formation of larger metal particles and modifies the activity and selectivity (growing chain). Acidity/basicity of the support modifies the selectivity; with a low acidity of the support (SiO_2 , Al_2O_3), linear products are obtained, but if support is too acidic (zeolites), branched alkanes or even aromatics are formed [87]. This is of interest for cobalt catalysts. For iron, potassium oxide is often added as promoter and the said problem is overcome. It is relatively difficult to distinguish between the effect of porosity and that of metal dispersion, the latter being modified by the sizes of the pores. However, it has been demonstrated on Co/ SiO_2 that the specific activity into methane decreases with the increase of pore diameter (4-20 nm) [88]. Same conclusions have been drawn on 2% Co/ Al_2O_3 [89].

The link between activity and type of support is quite difficult to establish. On cobalt (225 °C, 1 atm.), the specific activity is modified by the nature of the support: Co/ TiO_2 > Co/ SiO_2 > ~Co/ Al_2O_3 > Co/C > Co/MgO [90]. This has been attributed to a

different reduction stage of the cobalt [91] under the operating conditions. This change of state of reduction could be due to a partial reoxidation of Co° during the synthesis, which depends on the size of the metal particles, or to an incomplete reduction after catalyst activation related to the metal-support interactions. For the same kind of catalysts performing under pressure (5 bars, 200 °C), neither the specific activity nor the methane or C_{5+} selectivity is affected by the nature of the support [91].

12.5.4 Choice of the Promoters

Both iron and cobalt catalysts could be promoted by transition metals or by oxides. For cobalt, numerous metals such as Ru, Pt, Pd, and Re have been introduced during the preparation phase (impregnation) [70]. All the added metals (except Re) are easily reducible at low temperature (below the reduction temperature of the cobalt oxide Co_3O_4) [92,93]. The effect of Re oxide promotion on the reducibility of cobalt is generally less significant than with Ru, Pt, or Pd oxides. The temperature of Re oxide reduction occurs above the first step of Co_3O_4 reduction (CoO formation), and it was suggested that the presence of Re affected only the second reduction step (reduction of CoO to Co metal) [63]. Easy reducibility of the second metal favors chemisorptions of hydrogen at lower temperature than with cobalt alone and consequently their addition permits the decrease of the temperature of reduction and the increase of the reduction percentage of the cobalt oxide. Additionally, Pt and Pd could form an alloy or bimetallic particles with cobalt [94,95]. Other effects have been described: the change in cobalt dispersion (Pt, Pd) prevents catalyst deactivation, promotes activity, or modifies selectivity by the higher production of CH_4 (Ru). For iron catalysts, Cu is, historically, the added metal. It promotes the reduction of the iron oxides but also enhances the WGS reaction [96].

Promotion by oxides has also been largely used. On iron catalysts, addition of K_2O increases the basicity of the catalyst as well as CO and CO_2 adsorption. This increases both the growing chain and activity [57], but it also favors the WGS reaction. The WGS reaction, however, is suppressed by the addition of an alkali-earth element (Ca, Mg) [97]. Manganese oxide increases both activity and chain propagation. However, if MnO reacts with iron or cobalt oxides, a spinel structure is obtained and selectivity is directed to short-chain olefins [98,99]. The effect of the oxide promoter changes with the nature of the support. On SiO_2 , the benefit of ZrO_2 addition is the prevention of the formation of cobalt silicate, the increase in cobalt oxide reduction, and the modification of the ratio of the hexagonal/cubic cobalt phase (hexagonal phase being the most active) [71]. Added to alumina, ZrO_2 prevents CoAl_2O_4 formation, and increases the hexagonal/cubic ratio and cobalt dispersion, but decreases its reduction [100]. Rare-earth oxides (CeO_2 , La_2O_3) have often been used with essentially two effects: the covering of the active phase with a decrease in the chemisorption capacity, and the formation of new catalytic sites at the metal-promoter interface [101]. Reduced rare-earth oxides (CeO_2) are potential sites for CO adsorption with an easier C—O bond breaking [102]. At atmospheric pressure, on rare-earth-promoted Co/C catalysts, H_2 and CO adsorption is drastically reduced, but activity spectacularly enhanced ($\times 100$), with a better growing chain, olefin formation, and methane decrease [101,103]. Same conclusions have been drawn with promotion by V_2O_5 and MgO [104]. Such promotion has been attributed to localized interaction between promoters and the adsorbed species [48,105].

12.6 FT REACTORS

In conventional FT processes, four types of reactors are used:

- fixed-bed multitubular reactors
- fluidized-bed reactors
- slurry-bed reactors
- microchannel reactors.

Figure 12-13 illustrates schematically the principles of the four reactors [106]. The type of the reactor chosen to operate in the FT plant influences the parameters of the FT synthesis, the product distribution with chain growth probability, product selectivity, catalyst activity, and CO conversion [107,108].

12.6.1 Fixed-Bed Multitubular Reactor

Fixed-bed reactors are the oldest reactors installed and operated at commercial scale before and after Second World War in Germany. At the beginning, the catalyst was packed in a rectangular box, with cooling plates with water-cooled tubes being installed in the bed in order to remove the heat [109]. Afterward, the reactors were further developed, resulting in the multitubular fixed-bed reactor. This type of reactor was installed at the SASOL plant, South Africa in 1955, and was named Arge reactor (Figure 12-14). The reactor design comprised a

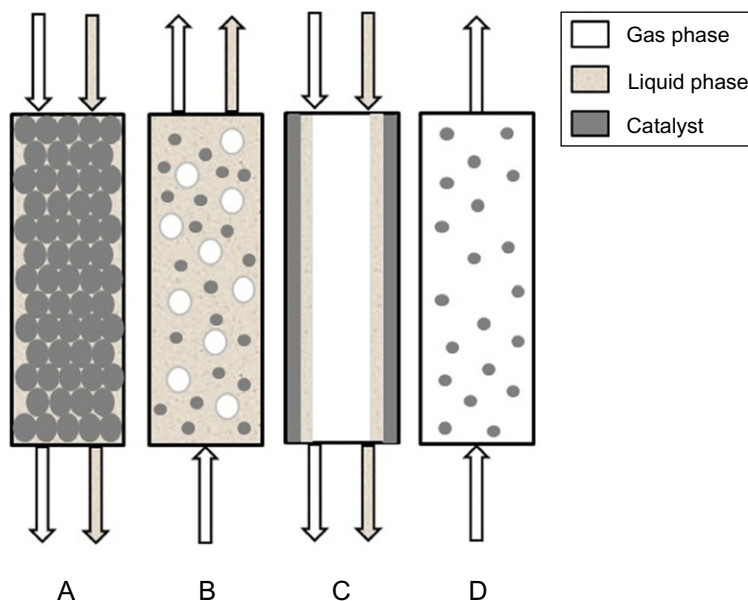


FIGURE 12-13 The principle of the Fischer-Tropsch reactors. (A) Fixed-bed reactor. (B) Slurry reactor. (C) Microchannel reactor. (D) fluidized reactor.

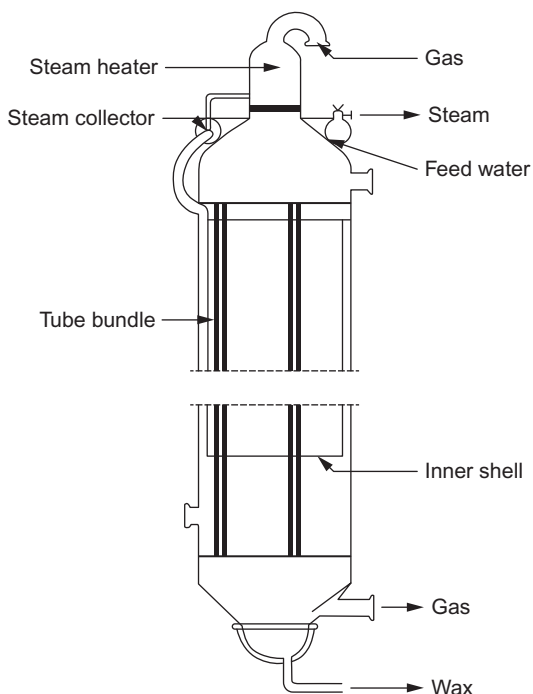


FIGURE 12-14 The Arge reactor.

shell containing 2050 tubes packed with an iron-based catalyst, and was 12 m high and 0.5 m in diameter. Heat removal from the FT synthesis was realized using steam on the shell side of the reactor. The normal operating conditions of the Arge reactor were as follows: temperature 220 °C, pressure 25 bar (for the reactor commissioned in 1955) and 45 bar (for the one commissioned in 1987, producing, respectively, 600 and 900 bbl/day/reactor [48]). Other similar reactors were designed and installed in the SMDS process at Bintulu Malaysia, in 1993, using a Co-based catalyst and producing products at the rate of 3000 bbl/day with an α value of around 0.9 and C_{5+} selectivity in the range of 85-95% [1,109]. SMDS process was also used in Las Raffan, Qatar, in the Pearl GtL facility, using a Co-based catalyst to produce products at 140,000 bbl/day [1].

Even though the fixed-bed multitubular reactors are robust and have high productivity, they have certain disadvantages, such as the following:

- design complexity, which is difficult to scale-up [48];
- high pressure drop, and insufficient heat removal due to poor heat conductivity [48,108,109];
- low catalyst utilization;
- requirement for the catalyst particles to be very small, in order to reduce the pressure drop and to facilitate the heat removal;
- filling of catalyst pores with heavy waxes due to diffusion limitation and capillary condensation [106];
- need for periodical replacement of catalyst, which is cumbersome [48];
- high cost [109].

12.6.2 Fluidized-Bed Reactors

Fluidized-bed reactors have been designed and commercialized in order to overcome the drawbacks and to improve the efficiency of fixed-bed reactors. This technology was developed only for the HTFT process because the FT synthesis has to occur entirely in the gas phase. Commercial fluidized-bed reactors include the bubbling fluidized-bed reactor (Figure 12-15B) and the CFB reactor (Figure 12-15A), both leading to similar product distributions [44].

The advantages of a fluidized-bed reactor, in comparison with a fixed-bed reactor, are as follows:

- superior heat transfer and temperature control during highly exothermic FT reactions [51,109];
- the possibility of using smaller catalyst particles, thereby avoiding intraparticle diffusion, which limits the reaction rate [109] and the pressure drop [51];
- better mixing of the catalyst particles due to fluidization and a higher gas-solid contact efficiency [51];
- easy replacement of the catalyst in a shorter time and the possibility of loading fresh catalyst during the run;
- high production capacity due to higher gas throughput [51].

However, the fluidized-bed reactor has some limitations too. It needs special equipment (cyclones) for catalyst separation, which can have an effect on the cost efficiency. Also, while using small catalyst particles, there is a high risk of attrition and of heavy product deposition

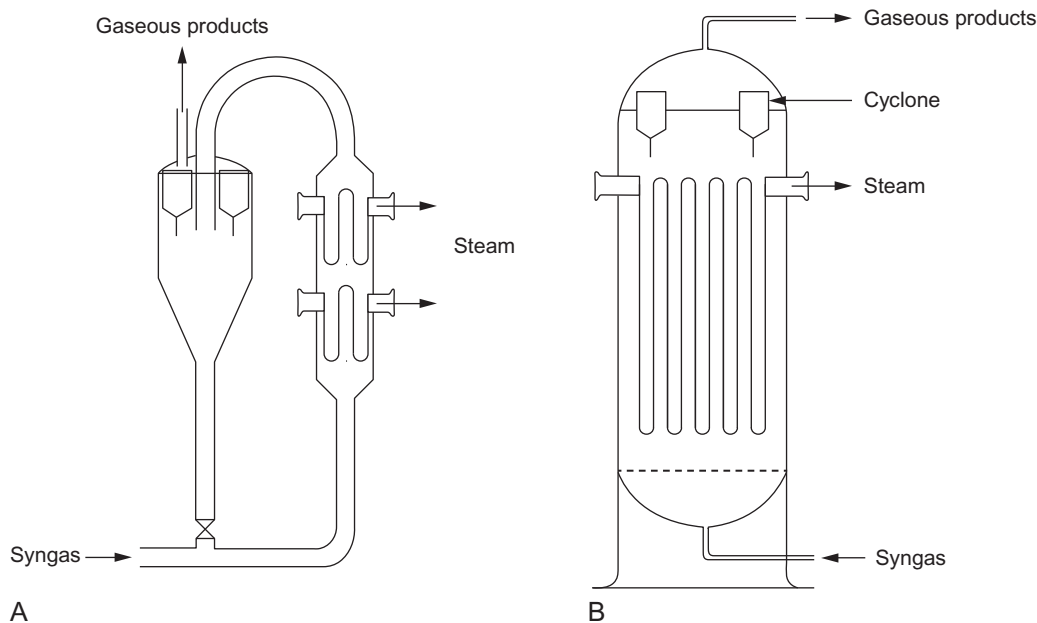


FIGURE 12-15 Fluidized-bed reactors. (A) Circulating fluidized. (B) Fixed fluidized.

on the catalyst, causing agglomeration and blockage of the fluidization [109]. Some important issues are the more complicated design and operation, difficulty in scale-up, and, usually, the necessity to develop scale-up strategies to predict gas hold-up, mass transfer between phases, and dense-phase backmixing, in order to avoid commercial design errors [51,109]. An example of these types of failures occurred when the pilot plant fluidized-bed reactor operated successfully with a conversion of over 95%, but reached a maximum of only 70%, which is uneconomical, when the technology was transposed to the industrial scale [110]. Hydrocol built a commercial plant in Brownsville using a fluidized-bed reactor with a diameter of 4 m, a height of 18 m, and a capacity of 180,000 t/year. But because of the technical and economic problems of the reactor, the plant was shut down in 1956 [109]. CFB reactors 2.3 m in diameter, 46 m in height, and having a capacity of 1500 bpd were also developed by SASOL during the 1980s. The technology was then switched to fixed-bed fluidized reactors because of their substantial reductions in scale—more compact for the same capacity, less energy required, and lower operating costs involved [109].

12.6.3 Slurry Reactors

Slurry reactors were developed to overcome the difficulties associated with the fixed-bed multitubular reactors. The first slurry reactor was commissioned by SASOL in 1993, with a diameter of 5 m and a height of 22 m (Figure 12-16) [48]. In 1990, at Exxon, LA, a 1.2 m diameter, 21 m high slurry reactor with a production capacity of 200 bbl/day was developed [109]. Compared to the fixed-bed multitubular reactor, the slurry reactor is much easier to design and much cheaper. Also, it has the advantage of fast heat removal and, because the slurry

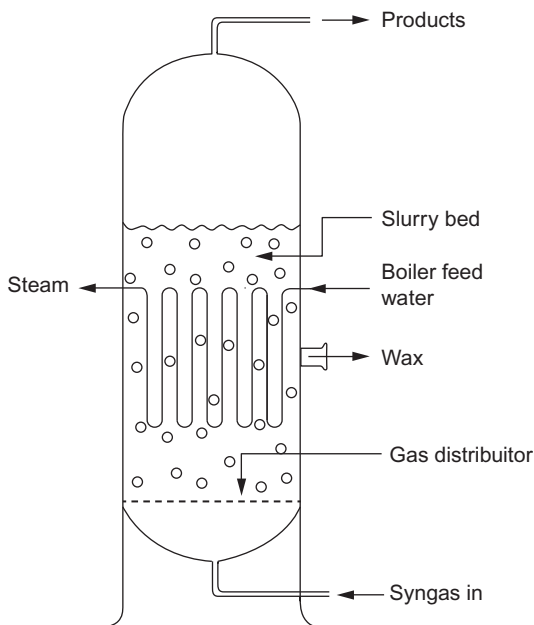


FIGURE 12-16 SASOL slurry-bed reactor.

phase is well mixed, the temperature inside the reactor is more constant (elimination of local hot spots) [48,111]. In this way, much higher temperatures on average can be achieved without the danger of sintering the catalyst. Increasing the slurry concentration will increase the formation of large bubbles, thereby enhancing the reactor productivity [112]. Other important advantages are the low pressure drop, the large catalyst area, easy removal of the catalyst, and lower catalyst consumption [16,48,113].

However, an important drawback of the slurry reactor is the separation of the catalyst from the waxes [16,37,108,109,112,113]. The catalyst for the slurry reactor is more susceptible to attrition. Due to the continuous circulation, the whole catalyst is exposed to the sulfur poisoning, unlike the case of fixed-bed reactors in which the top section acts as a guard bed. Espinoza *et al.* [114] showed that in a fix-bed reactor the mechanism of deactivation occurs differently in three regions of the reactor: In the top region, most of the catalyst particles are deactivated as a result of the sulfur trapped; in the middle region, they are less deactivated; and in the bottom region, almost no sulfur is found. Also, the scale-up of the reactor poses several problems due to the complex hydrodynamics, and a costly demonstration stage is necessary.

12.6.4 Microchannel Reactors

Recent advancement in chemical reactor technology has opened up new opportunities for FT synthesis in a new type of reactor—the microchannel reactor. These reactors consist of a large number of parallel channels with diameters below 1 mm and with the catalyst on a thin layer inside the channel walls. Even though, until now, no commercial FT plant has been using the microchannel reactor, this design allows for isothermal operation even for highly exothermic reactions [106,108,113] and improves mass and heat transfer, compared with conventional fixed-bed reactors. Cao *et al.* [108] compared the energy transfer and reactions in a microchannel and a conventional fixed-bed reactor, using a three-dimensional pseudo-homogeneous model. They demonstrated that, under the same operating conditions, large temperature gradients exist in the furnace-heated conventional fixed-bed reactor, while in the microchannel reactor, the catalyst showed a uniform temperature profile due to a high heat transfer coefficient between the bed and wall, large transfer surface area, and short transfer distance in the microchannel. Even at a GHSV of $60,000 \text{ h}^{-1}$ and temperature of $230 \text{ }^\circ\text{C}$, the temperature gradient of the reactor remained in a narrow range. Also, the microchannel reactor offers the best catalyst utilization and thus a high productivity.

It provides a promising route to the FT process and further research has to be conducted to improve its efficiency on the large scale. The main challenges of this reactor type are the difficulty in changing the catalyst and the significant investment required (almost no scale-up advantage regarding costs because for scaling up several microchannel reactors have to be operated in parallel).

12.7 REACTION CONDITIONS AT THE LABORATORY AND INDUSTRIAL SCALE

Catalysts play a crucial role in FT synthesis, with their preparation and reduction directly influencing the activity, CO conversion, and product selectivity. There are different ways for

the preparation and reduction of Fe- or Co-based catalysts. In the case of Fe-based catalysts, the preparation is mainly done with the precipitation method in combination with a spray-drying technique [48,111]. If the catalyst is used in a fixed-bed reactor, the preparation consists in a precipitation of $\text{Fe}(\text{NO}_3)_3$ solution and different promoter nitrates by an alkaline solution, and based on the precipitation temperature, rate of precipitation, concentration of the solutions, and order of addition, the surface area and the pore structure can be controlled. When the precipitation is complete, the precipitate is washed, filtered, and dried. The first commercial Fe-based catalyst was used at Hydrocol, Brownsville, USA, for the HTFT process. At typical operating conditions, temperature 305-345 °C and pressure 21-45 bar, the selectivity of the catalyst was for hydrocarbons in the naphtha range, with high concentrations of olefins, oxygenates, and aromatics [45]. Fe-based catalysts were later implemented by SASOL as well, not only for HTFT but also for LTFT in fixed-bed reactors. Significant attention has been devoted in the research field to the average crystallite size of Fe-based catalysts and promoters, which could improve the reduction temperature and thus the catalytic activity. Van Steen and Claeys [115] pointed out that a typical Fe-based catalyst (ARGE catalyst) contains several iron carbide phases and magnetite during FT operation conditions. The several phases present within the catalyst determine the average crystallite size. It is considered that the magnetite phase contains crystallites with sizes between 50 and 150 nm, while iron carbide species are much smaller (7-15 nm). This is due to the formation of magnetite species by iron carbide oxidation. Large particles of magnetite are not desirable in FT synthesis because of the breakage of the particles and their conversion back to the iron carbide species. At the same time, the small particles of iron carbide can sinter as a result of the water formation and become reoxidized, leading to the formation, again, of magnetite crystallites. All these transformations in the catalyst composition and structure might have a negative influence on the catalyst activity. Thus, promoters are often used in order to increase the catalytic performances of Fe catalysts. Potassium, copper, ruthenium, palladium, or platinum is used not only to enhance the activity of the catalyst but also to reduce the reduction temperature and to prevent the collapse of the highly porous iron oxides by calcination and reduction [115].

The same promoters are also used for Fe-based catalysts in slurry reactors. The precipitated catalyst is spray-dried because a much finer particle size is required in the slurry reactor [48]. Zhang *et al.* [116] demonstrated that the addition of Cu and K to the precipitated Fe-Mn/ SiO_2 provided more surface base to the catalyst, a lower reduction temperature, an increase in the reduction rate, and an accelerated activation of the catalyst.

Because of their ability to achieve high conversion, Co-based catalysts have become the most used catalysts for LTFT synthesis. The first commercial catalyst based on Co, ThO_2 , and kieselguhr was applied at Ruhrchemie and later at all the operation plants in Germany [117]. The catalyst was prepared by dissolving Co, Th, and Mg metals in nitric acid, followed by precipitation in the presence of soda and kieselguhr, filtration, drying, and crushing. The reduction of the catalyst was conducted at 400 °C in the presence of H_2 . Co-based catalysts have also been synthesized and reduced for LTFT at Shell, Exxon, and Chevron. In an attempt to minimize the amount of metal used, because of its high price, Co-based catalysts have been prepared by wet impregnation techniques on different supports (Al_2O_3 , SiO_2 , TiO_2 , zeolites, etc.). Also, to enhance the catalyst activity, different promoters (Ru, Re, Mo, Zr, Cr, La, alkali metals, etc.) can be impregnated after Co, using several steps of impregnation, in order to

achieve the desired composition. After impregnation, the catalyst is dried and calcined at a high temperature. At Shell, the preferred support for Co-based catalyst has been silica promoted with zirconium, titanium, or chromium. The typical preparation method was impregnation, in order to achieve 2-60 pbw (parts per weight) of Co and 0.1-150 pbw of Zr, Ti, Cr. Of all the promoters, Zr was found to improve most the catalytic performances of the Co-based catalysts [71]. The catalysts patented by Exxon contained 5-25 wt% Co dispersed on a TiO₂ support by impregnation. As promoters, Re, Ru have been used in the ratio Re/Co=0.025:1. In the case of the catalysts patented by Chevron, the typical supports used were γ - and η -Al₂O₃ or layered aluminosilicate impregnated with 1-50 wt% Co and Ru as promoter in the concentration 0.05-5 wt% [71].

Other promoters that have been used are Pt and Ir. It has been demonstrated that for a high degree of reduction and active sites, Co-based catalysts require the addition of promoters, especially in the case of catalysts that are difficult to reduce, such as cobalt aluminates, cobalt silicates, and cobalt titanates [115].

Different reduction steps are proposed in the literature for Fe- or Co-based catalysts, with a gradual increase in temperature and in the partial pressure of H₂ to minimize the negative effect of water produced during the reduction on the catalyst surface. A summary of different reduction parameters is presented in Table 12-6.

12.7.1 Operation Conditions

In commercial practice, there are two processes of the FT operation:

- LTFT (operation temperature 210-250 °C) developed in Germany in 1936 in the first FT industrial plant, and later in the Shell (Bintulu Malaysia), SASOL, and Oryx GtL (Lass Raffan, Qatar) plants;
- HTFT (operation temperature 310-340 °C) developed at the Cartage Hydrocol FT plant, USA (operation: 305-345 °C, 21-45 bar, bubbling fluidized bed); the SASOL I plant, which integrated HTFT (340 °C, 20 bar, CFB reactor) with LTFT (230 °C, 27 bar, bubbling fluidized-bed reactor); and SASOL Secunda; PetroSA, Mossel Bay, South Africa [1].

LTFT is the preferred technology for the production of FT diesel and waxes, instead of HTFT [122]. With the HTFT process, the products are shifted to light products (naphtha, alkenes, gasoline), while in the case of LTFT, the products consist of heavy, waxy hydrocarbons [44,123]. The different operation conditions used in LTFT and HTFT laboratory plants are listed in Table 12-7.

In the case of Fe-based catalysts, it has been demonstrated that operation conditions and promoters have an impact on the catalyst activity and selectivity. Alkali metals such as K, Mg, Na, and Li demonstrate not only a lower CH₄ selectivity but also an increase in the reaction rate, alkene selectivity, and chain growth probability. They also provide resistance to the catalyst against oxidation during the operating conditions, especially when it is in contact with the water produced in FT synthesis [114]. Zhang *et al.* [116,124] showed that the addition of Cu and Ni to the Fe-Mn-K/SiO₂ catalyst results in a reduction in the methane selectivity and an increase in heavy hydrocarbons, demonstrating that Cu promotes a chain propagation reaction as a result of the high basicity of the surface. On the other hand, increasing the H₂/CO

TABLE 12-6 Reduction Parameters for Fe and Co Catalysts

Catalyst	Reactor	Reduction agent	Temperature (°C)	Temperature ramp (°C/min)	Pressure (bar)	Space velocity (l·g ⁻¹ ·h ⁻¹)	Hours (h)
Fe/Cu/K/SiO ₂ [111]	Stirred-tank slurry reactor	Syngas H ₂ /CO=0.67	270	0.17	10-25	1	13
Fe-Mn ultrafine catalyst [112]	Stirred-tank slurry reactor	Syngas H ₂ /CO=2	275	-	35	1	32
Fe-Mn catalyst [113]	Stirred-tank slurry reactor	Syngas H ₂ /CO=1	280	-	15-20	0.23	48
Fe/Cu/La/SiO ₂ [53]	Fixed-bed reactor	5% H ₂ /N ₂ gas mixture	400	5	atm.	15.1	1
Fe-Mn catalyst [118]	Fixed-bed reactor	Syngas H ₂ /CO=2	400	-	25-30	1	32
FeCrAlY foam [51]	Microchannel reactor	5% H ₂ /He	350	-	atm.	-	12
Co-Ru/Al ₂ O ₃ [49]	Stirred-tank slurry reactor	H ₂	400	2	atm.	1.2	24
Co-Ru/Al ₂ O ₃ [52]	Fixed-bed reactor	H ₂	400	1	atm.	-	12
Co-Re/Al ₂ O ₃ [119]	Fixed-bed reactor	H ₂	350	1	1	-	16
Co-Re/Al ₂ O ₃ [71]	Fixed-bed reactor	H ₂	250-350	-	atm.	-	Overnight
Co-Re/Al ₂ O ₃ [120]	Fixed-bed reactor	H ₂ +He 1:2	Step 1: 100 Step 2: 350	Step 1: 2 Step 2: 1	atm.	-	1 10
Co-Pt/Al ₂ O ₃ [121]	Fixed-bed reactor	H ₂	350	-	atm.	-	8

TABLE 12-7 Operation Conditions for FT Synthesis

Catalyst	Reactor	Temperature (°C)	Pressure (bar)	H ₂ /CO	Space velocity (l·g ⁻¹ ·h ⁻¹)	CO conversion (%)
Fe-Mn ultrafine catalyst [112]	Stirred-tank slurry reactor	260-300	15-31	0.65-2	1-2.5	91-95
Fe-Mn catalyst [113]	Stirred-tank slurry reactor	260-290	9.3-25.3	0.8-2.5	1-6.6	60-80
Fe-Mn catalyst [118]	Fixed-bed reactor	280-340	22.5	1.01-2.74	0.8-5.6	64-88
Fe-Mn-K/SiO ₂ [116]	Slurry reactor	250	15	1.35-1.4	-	59-74
Fe-Mn-Cu-K/SiO ₂ [116]	Slurry reactor	250	15	1.35-1.5	-	62-76
Co-Ru/Al ₂ O ₃ [42]	Stirred-tank slurry reactor	210-240	20-35	1-2.5	0.5-1.5	
Co-Ru/Al ₂ O ₃ [44]	Fixed-bed reactor	210-240	25	0.5-2	0.448	
Co-Re/Al ₂ O ₃ [119]	Fixed-bed reactor	210	20	2.1	-	40-50
Co-Re/Al ₂ O ₃ [120]	Fixed-bed reactor	210	19.7	2	2	70-75
Co-Pt/Al ₂ O ₃ [121]	Slurry reactor	230	20	2	-	61.3

ratio between 1.3 and 1.4 (as can be seen in Table 12-7) results in an increase in the CO conversion but a reduction in heavy hydrocarbon selectivity as well due to a higher H₂ partial pressure, and, thus, more hydrogen species on the catalyst surface, which will hinder the combination of the carbon species.

The CO conversion of Co-based catalysts presented in Table 12-7 is influenced by the type of support and promoters, catalyst type, and operation conditions—temperature, pressure, space velocity, and H₂/CO ratio. Catalysts supported on SiO₂ and Al₂O₃ register higher CO conversion than TiO₂ due to the larger surface area available [115]. Xu *et al.* [121] demonstrated that Pt provides a higher enhancement of the CO conversion compared with Pd or Ru. Also, Pt improved the selectivity for heavy hydrocarbons and the reduction of CH₄ selectivity. Das *et al.* [120] demonstrated that CO conversion increases with Re promoter loading as a result of a higher reduction of Co.

Variations in the operation conditions of the FT synthesis influence the CO conversion, chain growth probability α , carbon distribution, and hydrocarbon selectivity toward light or heavy products, as given below:

- temperature: increasing the temperature results in an increase in CO conversion, CH₄ and C₂-C₄ selectivity, selectivity for olefins and oxygenates, and a decrease in C₅₊ selectivity

and α value. A high temperature results in a shift toward light hydrocarbons due to the increase in H_2 partial pressure inside the reactor, and thus more hydrogen species get on the catalyst surface, leading to chain termination and release of hydrocarbons; also, the olefins are hydrogenated and their chain propagation is suppressed [49,52,53,113,123,125,126];

- pressure: increasing the pressure can result in different behaviors. In some experiments, the product distribution was independent of the reaction pressure [53,113], while in others the increase in pressure resulted in an increase in CO conversion, C_{5+} selectivity, and α value, and a decrease in CH_4 and C_2 - C_4 selectivity [49,112,127]. An increase in CO conversion means that more C_1 intermediates get on the catalyst surface, increasing the rate of propagation and the chain growth;
- H_2/CO ratio: increasing the H_2/CO ratio results in an increase in CO conversion and selectivity of alkenes, and a decrease in the C_{5+} selectivity and α value due to the enhancement of H_2 species, which separate and hinder the combination of the carbon species [49,52,112–118];
- Space velocity: a higher space velocity results in a sharp decrease in CO conversion, due to a decrease in the residence time of the reactants and products. Regarding hydrocarbon selectivity, the effect of space velocity is variable; for instance, when using an Fe-based catalyst and a low H_2/CO ratio, the C_{5+} selectivity increased with an increase in the space velocity. Even though the residence time was lower, the effect of the low H_2/CO ratio was more pronounced, which favored chain growth [113,118]. On a Co-based catalyst and constant $H_2/CO=2$, the CH_4 selectivity decreased because of the negative influence of space velocity.

12.7.2 Aging of the Catalyst

Studying the deactivation of the catalyst during FT synthesis is a major challenge particularly in the case of cobalt-based catalysts. Iron-based catalysts are less sensitive to the synthesis gas quality (catalyst poisoning is less crucial). However, determining the origin of the deactivation is difficult. Several reasons could contribute to the loss of activity or selectivity, such as poisoning by sulfur and/or nitrogen-containing compounds in the synthesis gas feed; oxidation of the active metal cobalt to an inactive cobalt oxide; cobalt-support compound formation (silicates, aluminates); sintering of cobalt crystallites into larger ones and surface reconstruction; and carbon formation and attrition of catalyst particles. The given reasons for deactivation could be more or less pronounced according to the type of reactor, the nature of the support, and the syngas conversion (increase in the water partial pressure with an increase in conversion). Generally, the deactivation is due to a combination of several phenomena. Excellent analyses of the reasons for the deactivation of cobalt-based FT catalysts are available [128,129]. Most of the research (60% of the articles) in cobalt-based catalyst deactivation has been focused on cobalt oxidation, and only 14% on metal sintering [129].

Deactivation of the catalysts (loss of activity) in a demonstration plant could be described in two periods [130]. The first one corresponds to a reversible deactivation and lasts from some days to some weeks. The deactivation percentage could be high (20-40%)

[129,130]. The second period is a long-term, irreversible deactivation. However, better knowledge of the mechanisms of deactivation could initiate a successful regeneration procedure [129].

1. Poisoning by sulfur and nitrogen-containing compounds: Poisoning by the impurities of syngas is totally independent of the operating conditions and of the nature of the catalyst, and, if the severity of deactivation is high, the sulfur and nitrogen compounds can be removed from syngas. Cobalt-based catalysts are more sensitive to sulfur than iron-based catalysts; thus, additional gas cleaning steps are required in order to lower the sulfur content from 100 ppb (Fe) to 10 ppb (Co) [11]. It is also a fact that Co-based catalysts have a higher activity and a longer life time, but they are much more expensive than Fe-based catalysts. So removal of sulfur has to be more efficient. Sulfur adsorbs strongly on catalytic active sites, thereby physically blocking the sites. For a Co/Al₂O₃ catalyst, it has been shown that one adsorbed sulfur atom poisons more than two cobalt atoms [131]. The nature of sulfur (organic, inorganic) is important since the adsorption phenomena are different. In the case of H₂S, which is generally used as the probe molecule, studies agree on the negative effect on the catalytic activity and also on the catalyst selectivity. Directly linked to the high loading of H₂S, less CO conversion, less C₅₊ and C₂₅₊ hydrocarbons, and more CH₄ and C₂-C₅ hydrocarbons fraction are formed [132]. A negative effect on catalyst reducibility has also been reported. Removal of nitrogen compounds (NH₃, HCN) is also of prime importance. Concentration in the feed of less than 50 ppb has been proposed for syngas and methane on cobalt catalysts [133]. Fortunately, the deactivation appears to be reversible [129].
2. Reoxidation of cobalt: With cobalt catalysts, oxygen of CO (surface oxygen or OH species) is eliminated mainly as water during the FT synthesis, and a reoxidation of the metallic cobalt active sites is possible, especially at high CO conversion when the partial pressure of water is high compared to that of H₂ and CO. The effect of water has been well described in recent articles [42,134,135]. The stability diagram of bulk cobalt metal and cobalt oxides shows clearly that reoxidation of metallic cobalt is not feasible under FT conditions, but thermodynamic calculations have demonstrated the possible oxidation of spherical cobalt particles of less than 4.4 nm if CO conversion is high (75% conversion, $T = 220\text{ }^{\circ}\text{C}$) [136]. The discussion on the possible reoxidation of cobalt metal particles is still under controversy. Numerous studies—not always in the true FT operating conditions (e.g., addition of water)—have indicated a possible reoxidation of the surface depending on the operating conditions and cobalt dispersion [137,138]. The effect of water on reoxidation is also strongly related to the nature of the support (Al₂O₃, SiO₂, TiO₂), on the presence of the promoter (Re, Pt), and on the size of the pores of the support. As an example, a study on Co/SiO₂ was carried out in a simulated FT environment with different cobalt crystallite sizes (4, 13, 28 nm). The smallest crystallites were resistant to oxidation, while particles of 13 nm were largely oxidized (30%), and on crystallites of 28 nm, less than 2% oxidation was found [139]. On alumina (Co-Pt/Al₂O₃ catalyst) in industrial FT conditions, XANES analyses of 6-nm average cobalt crystallites showed a significant increase in the fraction of metallic cobalt. So the authors concluded that deactivation was not due to reoxidation for cobalt particles larger than 6 nm or even 2 nm, as reported in another study [129,136,140]. It was also demonstrated in hydrothermal FT conditions that the presence of water induces

phase transformation with cobalt-silica mixed oxide formation [141,142]. Formation of cobalt-alumina mixed oxides was also indicated and related to reoxidation of cobalt. Reoxidation increases the mobility of cobalt crystallites and assists in the formation of inactive mixed oxides, but leads to sintering as well. Another explanation for Co/SiO₂ or Co/Al₂O₃ catalysts, based on revised thermodynamic calculations, is that mixed compounds are formed from unreduced cobalt oxide and not from cobalt that was oxidized [129]. The presence of water favors hydration of alumina, which enhances the diffusion of small CoO particles. The conclusion of Saib *et al.* [129] was that, under realistic FT conditions, reoxidation does not occur for cobalt crystallites larger than 2 nm. This was supported by the work of the same group [135,136,139,140] and that of other groups [143–146].

3. Sintering: Sintering is, in metal catalysis, a common mechanism of deactivation and is based on the surface energy minimization of the crystallites. This process is favored by high temperature and water vapor but decelerated by interactions with the metal support. It depends on the size of the metal crystallite. Generally, sintering is considered as an irreversible phenomenon; however, with the reduction-oxidation-reduction (ROR) sequence, it may be possible to redispense the catalyst and to restore the initial activity. Commercial Co/Pt/Al₂O₃ catalysts have been studied after use in a slurry bubble column reactor [129,140,147]. By transmission electron microscopy (TEM), it was demonstrated that initially cobalt, in crystallite sizes of between 3 and 15 nm (maximum abundance 6 nm, average size 9.5 nm), is located in larger grape-like regions (100 nm) well distributed on the alumina support. After 20 days, TEM showed an increase in the crystallite size from 9.5 to 15 nm occurring in the first 15 days and a partial disappearance of the grape-like feature. With a direct correlation between activity and cobalt metal surface, it has been calculated that the contribution of sintering is about 30% of the observed loss in activity [129]. After the ROR sequence, the grape-like features are again visible in the small cobalt particles. Activity is totally recovered but ROR regeneration includes both redispersion of the metal and oxidation of the deposited carbon, and total recovery of activity cannot be attributed solely to the redispersion of cobalt particles. On Co-Re-Al₂O₃ catalysts, tested under relevant conditions, synchrotron X-ray diffraction showed no increase in particle size at 210 °C after 2 h, but there was an increase of 20% with an increase in temperature to 400 °C. Another study on Co/Al₂O₃ showed an increase from 6 to 10 nm of fcc (face-centered cubic) Co crystallites at 210 °C, 20 bar [148]. The group of Davis [120,149,150] showed with extended X-ray absorption fine structure an increase from 2.7 to 7.6 in the coordination number of the first Co-Co shell, suggesting the sintering of the cobalt clusters in a Co-alumina promoted (Re) catalyst. The same trend was found when cobalt was promoted by Pt or Ru. Sintering of cobalt may be accelerated by the presence of water [151]. As an example, de Smit and Weckhuysen [152] observed by TEM the sintering of cobalt crystallites from 5 to 11 nm (220 °C, 35 bar, 10 bar steam), and Bian *et al.* [145] also showed sintering for a Co/SiO₂ catalyst (240 °C, 10 bar, 90% CO conversion). Coalescence is proposed as the predominant sintering mechanism.
4. Carbon formation: Carbon formed by CO dissociation is the reactive intermediate species in the FT reaction. If the hydrogenating power of the catalyst is too low, part of this carbon could be transformed into a more stable carbon with a gradual transformation to

polymeric carbon, which could contain some hydrogen atoms, and then finally to graphitic carbon. Carbon bound irreversibly to active sites has a detrimental effect on the FT reaction. Other possibilities are the reactions with active metals to form iron or cobalt carbides or the electronic modification of the metallic phase. The probability of bulk cobalt carbide is low compared to that of iron carbides. In fact, the diffusion rate of carbon in cobalt is 105 lower than in iron [152]. Some authors [152–154] have attributed the deactivation of catalysts to the carbidization of bulk cobalt. However, it has been shown that hydrogenation of bulk cobalt carbide leads to the formation of a cobalt structure (hexagonal close-packed cobalt structure), which is highly active in the FT process [155]. Carbon deposited on the support is not considered to decrease the catalytic activity. Carbon on the catalytic surface could also originate from side reactions: namely, decomposition of CO by the Boudouard reaction, or decomposition of already formed high molecular weight hydrocarbons ($C > 100$). Such hydrocarbons block parts of the pores and of the catalytic surface (high residence time), lose part of their hydrogen atoms, and transform progressively into coke or graphite-like species [156]. It has been suggested that the initial deactivation could be a result of the selective blockage of the smallest pores [157]. By temperature programmed hydrogenation or/and oxidation, different carbonaceous species have been characterized on a Co-Pt/ Al_2O_3 tested under industrial conditions [158]. Peaks at ~ 250 , 340, and 430 °C correspond to carbon species hydrogenation. The last one, less reactive for hydrogenation in CH_4 , was identified as polymeric carbon [158]. The amount of polymeric carbon is proportional to the time on stream, and was postulated as the main cause of the low decrease in activity in the long run (second part of the deactivation curve). Another possibility of the carbon surface evolution is its diffusion into the first subsurface layer (thermodynamically favorable) [129]. The presence of subsurface carbon is likely to reduce CO adsorption and dissociation on nearby atoms. Finally, surface carbon could be involved in the process of metallic surface reconstruction observed under a syngas environment [159] between fcc Co(100) and fcc Co(111) faces. A number of studies are indirectly related to surface reconstruction, especially studies showing that activity increases after some days on stream until the catalysts reach the most active FT structure [160,161].

5. Attrition of catalyst particles: Attrition is more intense in fluidized- or slurry-bed reactors, and the mechanical strength of the support and of the metal loading are critical parameters: $Al_2O_3 > TiO_2$ (rutile) $> SiO_2$ [162]. Abrasion or fragmentation of catalyst particles may result in catalyst loss, production of fine particles, and modification of fluidization properties with catalyst deactivation.

12.8 MECHANISM OF FT REACTIONS

The mechanism of carbon-carbon bond formation in FT synthesis has been the subject of extensive study for over 80 years. An understanding of the surface chemistry at the molecular level is seen by many researchers as essential for scientific understanding and maybe to improve the design of future catalysts. However, as indicated recently [11], there

is no evidence that catalysts have been developed on the basis of a given mechanism. The mechanism has been the subject of long academic studies, and has been reviewed extensively [163–170]. This is due mainly to the complexity of the CO chemistry and to the broad product range (number of carbons involved and chemical nature of the formed products). Although the formed hydrocarbons are, in a first approach, in agreement with a polymerization model (the ASF model), the process is not a simple polymerization reaction. The main difference with a polymerization is that the monomer(s) has to be synthesized *in situ* from CO and H₂ on the surface of the catalysts. This is why knowledge of the nature of the active species on the catalytic surface seems to be so important. A great number of mechanistic schemes have been proposed where the fundamental differences, as well as the nature of the monomer and of the initial active species, are being investigated. Most supported mechanistic proposals are briefly described in the following paragraph.

The first one is the hydrogenation into the CH₂ (CH_x) group of the carbided metal surface [10,171], the metal surface (M) being carbided by gaseous CO. It has subsequently been slightly modified, and involves, first, a C—O bond dissociation into carbon and oxygen surface species. Surface carbon then reacts with chemisorbed hydrogen atoms to form a C₁ intermediate species M-CH_x. The oxygen adsorbed is eliminated from the surface by reaction with adsorbed hydrogen (water formation on cobalt catalyst) or with adsorbed carbon monoxide (CO₂ formation on iron catalyst). The M-CH_x species reacts with another M-CH_x species for a growing chain via insertion of a CH_x group into the metal-carbon bond of the second entity. This mechanism remains the most accepted, and FT synthesis is considered to proceed via the formation of surface carbide, hydrogenation into methylene species, and then polymerization. Finally, the chain termination and the hydrocarbon formation are realized by hydrogenation of the surface alkyl group (paraffins formation) or by β-elimination of hydrogen (olefin formation). Some authors have proposed a reaction between the surface methylene and methyl groups for the growing chain [167]. The most important aspect of this proposal was to demonstrate the presence and the reactivity of carbene species. Studies using diazomethane [172] or chlorinated hydrocarbons [173] or cofed alkenes [174] have given strong arguments to support the participation of CH_x species in FT synthesis by changing the carbene species concentration at the catalyst surface. However, the oldest studies with precarbided ¹⁴C catalyst showed little incorporation of ¹⁴C isotope in the ¹²CO/H₂ reaction [175].

With ketene as probe molecule [176], it was observed that the CH₂ group did not participate in chain growth. This could indicate that all the added CH₂ groups might have significantly different states of absorption compared to CH₂ derived from CO hydrogenation. The characterization of such carbene has also been obtained directly by IR [177] or ¹³C NMR [178], by scavenging of alkyl species by pyridine [179] under CO/H₂ conditions, or by model studies using organometallic complexes [169,180,181]. So there is a considerable amount of data to support the carbide mechanism (Figure 12-17); but several objections remain, mainly the fact that the mechanism never explains either the branched isomer formation or the formation of oxygenated by-products (acids, alcohols, ketones, and aldehydes), especially on iron catalysts. It is also true that the evidence for the carbide mechanism could be interpreted in other ways, especially if we take into account the differences in the activity of CH₂ species coming from different precursors [169,173].

CO dissociation and hydrogenation

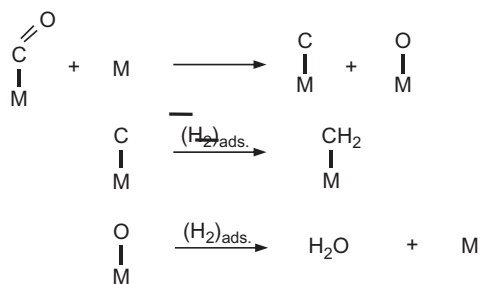
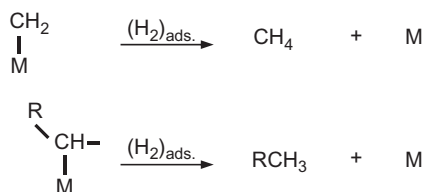


FIGURE 12-17 Carbide mechanism.

Polymerization



Desorption (chain termination)



The second developed mechanism (Figure 12-18) is based on the hydroxycarbene species (CHOH) as intermediates [163,166]. CO is associatively adsorbed on the surface, and then partly hydrogenated into hydroxycarbene species. C—C bond formation occurs from the condensation of two hydroxycarbenes with water elimination. The mechanism is consistent with studies using CO-fed alcohols, which indicate that oxygenated surface intermediates are incorporated in the chain growth [181]. However, some differences have been found based on the nature of the catalyst (Fe or Co) [164,168]. But the main problem remains in the explanation of the self-reaction of two hydroxycarbenes to form the carbon-carbon bond.

The third proposal involves CO insertion into a metal-alkyl bond (Figure 12-19) [182–184]. The resulting acyl species could be transformed by hydrogenation into oxygenates or hydrocarbons. Although evidence has been provided that clearly indicates that insertion of CO into metal-hydride or metal-alkyl is feasible [185,186], little experimental support exists for hydrocarbon formation in heterogeneous catalysis following this mechanism.

The three mechanisms discussed involve only one active species as a chain growth intermediate, namely, CH₂, CHOH, or CO, and each proposal has difficulty explaining the full product FT distribution. This is why some authors propose several intermediates: CH₂ and CO to explain the obtained products, and two independent pathways for hydrocarbon and alcohol formation [62,167,174]. Finally, there appears to be a consensus that more than one active species may be present on the catalytic surface.

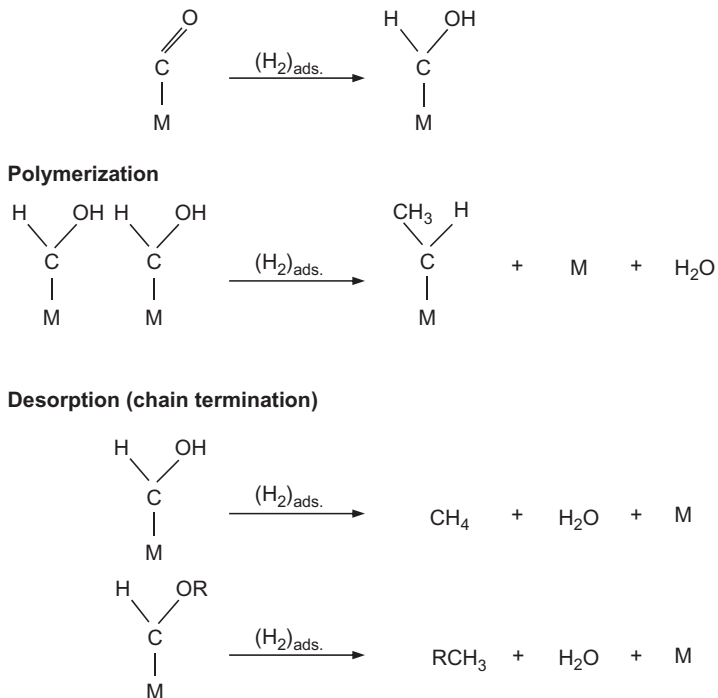


FIGURE 12-18 Hydroxycarbene mechanism.

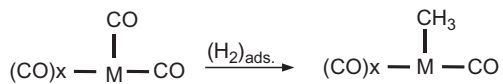
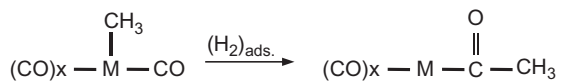
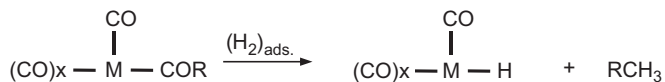
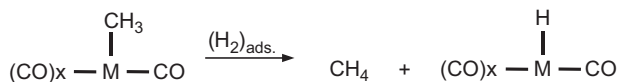
Reduction of adsorbed CO**Polymerization****Desorption (Chain termination)**

FIGURE 12-19 CO insertion mechanism.

12.9 CONCLUSIONS

BtL technology plays an important role in the sustainable energy policies, and FT synthetic transportation fuels are a promising alternative to conventional ones. Based on the investigations carried out, the following conclusions can be drawn:

- Biomass represents an attractive alternative energy feedstock for synthesis gas production followed by FT reaction but offers the greatest challenge to the development of gasification systems due to the lower concentration of contaminants compared to coal.
- Different types of gasifiers can be used for biomass conversion to syngas. Fluidized bed, entrained flow, and dual fluidized bed are now considered as the most efficient processes.
- Biomass gasification plants for the production of biofuels are under development in Austria, Germany, Finland, Sweden, Netherlands, Canada, and the United States.
- Syngas produced from biomass has a totally different composition compared to syngas from natural gas, with a lower H_2/CO ratio and more contaminants, requiring more gas cleaning stages.
- With the existing gas cleaning technologies, namely, wet cold and hot dry gas cleaning, the synthesis gas can achieve the low concentration of contaminants required by FT synthesis.
- FT reactors have to be chosen not only from the product selectivity point of view, but also from the economic viewpoint.
- Slurry reactor and microchannel reactors offer the best catalyst utilization and productivity, but further research has to be conducted in order to enhance their efficiency.
- Reaction kinetics and mechanisms show the complexity of the FT reaction in dissociating CO and addition of H_2 and C on the active surface for chain growth.
- Reduction and operation conditions of the catalyst play crucial roles in the FT synthesis, activity of the catalyst, and product distribution, and small changes result in significant deviations in CO conversion, chain growth probability, hydrocarbon distribution, and selectivity.
- Deactivation of the catalyst is inevitable, and therefore regeneration and promotion of the catalyst has to be done to achieve a longer life time of the catalyst and more efficiency of the FT synthesis.

References

- [1] D. Leckel, *Energy Fuel* 23 (2009) 2342–2358.
- [2] A. Demirbas, *Biodiesel: A Realistic Fuel Alternative for Diesel Engines*, Springer Publishing, London, England, 2008. ISBN: 978-184628-994-1.
- [3] A.P.C. Faaij, *Energy Policy* 34 (2006) 322–342.
- [4] P. Havlik, U.A. Schneider, H. Böttcher, S. Fritz, R. Skalsky, K. Aoki, S. De Cara, G. Kindermann, F. Kraxner, S. Leduc, I. McCallun, A. Mosnier, T. Sauer, M. Obersteiner, *Energy Policy* 39 (2011) 5690–5702.
- [5] A. Ajanovic, R. Haas, *Energy* 35 (2010) 3340–3348.
- [6] P. Sabatier, J.B. Senderens, *C. R. Acad. Sci.* 134 (1902) 514.
- [7] German Patent 293787 assigned to BASF (1913).
- [8] F. Fischer, H. Tropsch, *Brennst. Chem.* 4 (1923) 276.
- [9] F. Fischer, H. Tropsch, German Patent 2184337 (1985).
- [10] F. Fischer, H. Tropsch, *Brennst. Chem.* 7 (1926) 97.

- [11] M.E. Dry, Handbook of Heterogeneous Catalysis, in: G. Ertl, H. Knözinger, F. Schüth, J. Weitkamp (Eds.), Sec. Edition, Wiley-VCH Weinheim, 2008, pp. 2965–2992 Chap.13.15.
- [12] T.J. Remans, G. Jenzer, A. Hoek, Handbook of Heterogeneous Catalysis, in: G. Ertl, H. Knözinger, F. Schüth, J. Weitkamp (Eds.), Sec. Edition, Wiley-VCH Weinheim, 2008, pp. 2994–3010 Chap.13.15.
- [13] Y. Lu, T. Lee, *J. Nat. Gas Chem.* 16 (2007) 329–341.
- [14] D. Kilanowski, <http://www.velocys.com/news/conferences.php>.
- [15] Kr. Göransson, U. Söderlind, J. He, W. Zhang, *Renew. Sustain. Energy Rev.* 15 (2011) 482–492.
- [16] M.J.A. Tijmensen, A.P.C. Faaij, C.N. Hamelinck, M.R.M. van Hardeveld, *Biomass Bioenergy* 23 (2002) 129–152.
- [17] C.G. Visconti, L. Lietti, E. Tronconi, P. Forzatti, R. Zennaro, S. Rossini, *Catal. Today* 154 (2010) 202–209.
- [18] C.G. Visconti, E. Tronconi, L. Lietti, R. Zennaro, P. Forzatti, *Chem. Eng. Sci.* 62 (2007) 5338–5343.
- [19] D. Tristantini, S. Lögdberg, B. Gevert, Ø. Borg, A. Holmen, *Fuel Proc. Technol.* 88 (2007) 643–649.
- [20] H. Hellsmark, S. Jacobsson, *Energy Policy* 41 (2012) 507–518.
- [21] P. Lv, Z. Yuan, C. Wu, L. Ma, Y. Chen, N. Tsubaki, *Energy Convers. Manage.* 48 (2007) 1132–1139.
- [22] R. García, C. Pizarro, A.G. Lavín, J.L. Bueno, *Bioresour. Technol.* 103 (2012) 249–258.
- [23] V. Strezov, B. Moghtaderi, J.A. Lucas, *Biomass Bioenergy* 27 (2004) 459–465.
- [24] A. Faail, R. Vanree, L. Waldheim, *Biomass Bioenergy* 12 (1997) 387–417.
- [25] T. Chmielniak, M. Sciazko, *Appl. Energy* 74 (2003) 393–403.
- [26] C. Pfeifer, B. Puchner, H. Hofbauer, *Chem. Eng. Sci.* 64 (2009) 5073–5083.
- [27] A.K. Rajvanshi, *Alternative Energy in Agriculture*, CRC Press, Boca Raton, 1986, pp. 83–102.
- [28] S. Rapagnà, K. Gallucci, M. Di Marcello, M. Matt, M. Nacken, S. Heidenreich, P.U. Foscolo, *Bioresour. Technol.* 101 (2010) 7123–7130.
- [29] C.N. Hamelinck, A.P.C. Faaij, *J. Power, Sources* 111 (2002) 1–22.
- [30] A. Sauciu, A. Potetz, G. Weber, R. Rauch, H. Hofbauer, L. Dumitrescu, *International Conference on Renewable Energies and Power Quality ICREPQ 2011*, Gran Canary, Spain, 2011. ISBN: 978-84-614-7527-8.
- [31] A. Sauciu, Z. Abosteif, A. Potetz, G. Weber, R. Rauch, H. Hofbauer, G. Schlaub, L. Dumitrescu, *Environ. Eng. Manage. J.* 10 (2011) 1325–1334.
- [32] <http://www.choren.com/en/>.
- [33] <http://www.cutec.de/en/index.php>.
- [34] <http://www.westinghouse-plasma.com/>.
- [35] Y.H. Kim, K.W. Jun, H. Joo, C. Han, I.K. Song, *Chem. Eng. J.* 155 (2009) 427–432.
- [36] G. Higman, M. vanderBurgt, *Gasification*, Elsevier, Amsterdam, 2003. 402 pp.
- [37] N. Rados, M.H. Al-Dahhan, M.P. Dudukovic, *Ind. Eng. Chem. Res.* 44 (2005) 6086–6094.
- [38] M. Bremaud, P. Fongarland, J. Anfray, S. Jallais, D. Schweich, A.Y. Khodakov, *Catal. Today* 106 (2005) 137–142.
- [39] T. Riedel, M. Claeys, H. Schulz, G. Schaub, S.S. Nam, *Appl. Catal. A Gen.* 186 (1999) 201–213.
- [40] M.K. Gnanamani, W.D. Shafer, D.E. Sparks, B.H. Davis, *Catal. Commun.* 12 (2011) 936–939.
- [41] M.P. Aznar, M.A. Caballero, J. Gil, J.A. Martin, J. Corella, *Ind. Eng. Chem. Res.* 37 (1998) 2668–2680.
- [42] A.K. Dalai, B.H. Davis, *Appl. Catal. A Gen.* 348 (2008) 1–15.
- [43] L. Nowicki, S. Ledakowicz, D.B. Bukur, *Chem. Eng. Sci.* 56 (2001) 1175–1180.
- [44] A. Klerk, E. Furimsky, *RSC Catal. Ser.* 4. RCS Publishing ISBN: 9781849730808. (2010) 1–294.
- [45] A.P. Steynberg, M.E. Dry, *Fischer-Tropsch Technology*, Studies and Surface Science Catalysis, vol. 152, Elsevier, Amsterdam, 2004. 689 pp.
- [46] L. Tian, C.F. Huo, D.B. Cao, Y.Y. Yang, J. Xu, B.S. Wu, H.W. Xiang, Y.Y. Xu, Y.W. Li, *J. Mol. Struct.* 941 (2010) 30–35.
- [47] M. Ojeda, R. Nabar, A.U. Nilekar, A. Ishikawa, M. Mavrikakis, E. Iglesia, *J. Catal.* 272 (2010) 287–297.
- [48] B. Jager, R. Espinoza, *Catal. Today* 23 (1995) 17–28.
- [49] A. Sari, Y. Zamani, S.A. Taheri, *Fuel Proc. Technol.* 90 (2009) 1305–1313.
- [50] I.C. Yates, C.N. Satterfield, *Energy Fuel* 5 (1991) 168–173.
- [51] Y. Chin, J. Hu, C. Cao, Y. Gao, Y. Wang, *Catal. Today* 110 (2005) 47–52.
- [52] A. Tavasoli, A.N. Pour, M.G. Ahangari, *J. Nat. Gas Chem.* 19 (2010) 653–659.
- [53] A.N. Pour, Y. Zamani, A. Tavasoli, S.M.K. Shahri, S.A. Taheri, *Fuel* 87 (2008) 2004–2012.
- [54] I. Puskas, R.S. Hurlbut, *Catal. Today* 84 (2003) 99–109.
- [55] T.J. Donnelly, I.C. Yates, C.N. Satterfield, *Energy Fuel* 2 (1988) 734–739.
- [56] G. Broden, T.N. Rhodin, C. Brucker, R. Benbow, Z. Hurych, *Surf. Sci.* 59 (1976) 593–611.

- [57] T.J. Remans, G. Jenzer, A. Hock, *Handbook of Heterogeneous Catalysis*, second ed., pp. 2994-3010 (Chapter 13.16).
- [58] F. Fischer, H. Tropsch, P. Diltthey, *Brennst. Chem.* 6 (1925) 265.
- [59] M.A. Vannice, *J. Catal.* 37 (1975) 449-461.
- [60] M.A. Vannice, *Catal. Rev.* 14 (1976) 153-191.
- [61] M.E. Dry, *Catal. Today* 71 (2002) 227-241.
- [62] M.E. Dry, *Catal. Today* 6 (1990) 183-206.
- [63] H.H. Storck, *Fischer-Tropsch and Related Synthesis*, Wiley, New York, 1951.
- [64] H.W. Gross, et al. (to Ruhrchemie) German Patent 919288 (October 18, 1954).
- [65] W. Rottig (to Ruchchemie) German Patent 923128 (February 3, 1955) and US Patent 2777823 (January 15, 1957).
- [66] A.P. Steynberg, M.E. Dry (Eds.), In: *Studies in Surface Science and Catalysis*, vol. 152, Elsevier, Amsterdam, 2004.
- [67] M.E. Dry, in: J.R. Anderson, M. Boudart (Eds.), *Catalysis: Science and Technology*, vol. 1, Springer-Verlag, Berlin, 1984, pp. 159.
- [68] H. Koelbel, et al. (to Rheinpreussen Akt) German Patent 914969 (July 12, 1954).
- [69] Ruhrchemie German Patent 972900 (October 29, 1959).
- [70] A.Y. Khodakov, W. Chu, P. Fongarland, *Chem. Rev.* 107 (2007) 1692-1744.
- [71] R. Oukaci, A.H. Singleton, J.G. Goodwin, *Appl. Catal. A Gen.* 186 (1999) 129-144.
- [72] H. Ming, B.G. Baker, *Appl. Catal. A Gen.* 123 (1995) 23-36.
- [73] P.A. van Berge, J. van de Loosdrecht, E. Caricato, S. Barradas, B.H. Sigwebela, US Patent 6455462 B2 (2002).
- [74] A.A. Khasin, T.M. Yurieva, V.V. Kaichev, V.I. Bukhtiyarov, A.A. Budneva, E.A. Paukshtis, V.N. Parmon, *J. Mol. Catal. A* 175 (2001) 189-204.
- [75] Ph. Courty, C. Marcilly, *Rev. Inst. Fr. Pet.* 39 (1984) 445.
- [76] B. Ernst, A. Bensaddik, L. Hilaire, P. Chaumette, A. Kiennemann, *Catal. Today* 39 (1998) 329-341.
- [77] K. Okabe, X. Li, M. Wei, H. Arakawa, *Catal. Today* 89 (2004) 431-438.
- [78] S.L. Soled, E. Iglesia, R.A. Fiato, J.E. Baumgartner, H. Vroman, S. Miseo, *Top. Catal.* 26 (2003) 101-109.
- [79] E. Iglesia, S.L. Soled, R.A. Fiato, *J. Catal.* 137 (1992) 212-224.
- [80] E. Iglesia, *Appl. Catal. A* 161 (1997) 59-78.
- [81] G.L. Bezemer, J.H. Bitter, H.P.C.E. Kuipers, H. Oosterbeek, J.E. Holewijn, X. Xu, F. Kapteijn, A.J. van Dillen, K.P. de Jong, *J. Am. Chem. Soc.* 128 (2006) 3956-3964.
- [82] A. Gavriilidis, A. Varma, M. Morbidelli, *Catal. Rev. Sci. Eng.* 35 (1993) 399-456.
- [83] A.J. van Dillen, R.J.A.M. Terörde, D.J. Lensveld, J.W. Geus, K.P.J. De Jong, *J. Catal.* 216 (2003) 257-264.
- [84] E. Iglesia, S. Soled, J.E. Baumgartner, S.C. Reyes, *J. Catal.* 153 (1995) 108-122.
- [85] T.A. Nijhuis, A.E.W. Beers, T. Vergunst, I. Hoek, F. Kapteijn, J.A. Moulijn, *Catal. Rev. Sci. Eng.* 43 (2001) 345-380.
- [86] A.M. Hilmen, E. Bergene, O.A. Lindvag, O. Schanke, S. Eri, A. Holmen, *Catal. Today* 69 (2001) 227-232.
- [87] S. Bessel, *Appl. Catal. A Gen.* 96 (1993) 253-268.
- [88] J.A. Lapszewicz, H.J. Loeh, R. Chipperfield, *J. Chem. Soc. Chem. Comm. Issue11* (1993) 913.
- [89] D. Vanhove, Z. Zhuong, L. Makambo, M. Blanchard, *Appl. Catal.* 9 (1984) 327.
- [90] R.C. Reuel, C.H. Bartholomew, *J. Catal.* 85 (1984) 78-88.
- [91] E. Iglesia, S. Reyes, R.J. Madon, S.L. Soled, *Adv. Catal.* 39 (1993) 221.
- [92] L. Guzzi, D. Bazin, I. Kovacs, L. Borko, Z. Schay, J. Lynch, P. Parent, C. Lafon, G. Steffler, Z. Koppány, I. Sajo, *Top. Catal.* 20 (2002) 129-139.
- [93] N. Tsubaki, S. Sun, K. Fujimoto, *J. Catal.* 199 (2001) 236-246.
- [94] M.J. Dees, V. Ponc, *J. Catal.* 119 (1989) 376-387.
- [95] B. Mierzwa, Z. Kaszkus, B. Morawek, J. Pielaszek, *J. Alloys Compd.* 286 (1999) 93-97.
- [96] R.J. O'Brien, B.H. Davis, *Catal. Lett.* 94 (2004) 1-6.
- [97] M. Luo, B.H. Davis, *Appl. Catal. A Gen.* 246 (2003) 171-181.
- [98] J.J. Venter, M. Kaminsky, G.L. Geoffroy, M.A. Vannice, *J. Catal.* 103 (1981) 450-465.
- [99] G.J. Hutchings, M. van der Riet, R. Hunter, *J. Chem. Soc. Faraday Trans. I* 85 (1989) 2875.
- [100] G. Jacobs, T.K. Das, Y. Zhang, J. Li, G. Racoillet, B.H. Davis, *Appl. Catal. A Gen.* 333 (2002) 263-281.
- [101] J. Barrault, A. Guilleminot, J.C. Achard, V. Paul-Boncour, A. Percheron-Guegan, *Appl. Catal.* 21 (1986) 307.
- [102] J.S. Rieck, A.T. Bell, *J. Catal.* 96 (1985) 88.

- [103] J. Barrault, A. Guilleminot, J.C. Achard, V. Paul-Boncour, A. Percheron-Guegan, L. Hilaire, M. Coulon, *Appl. Catal.* 22 (1986) 273.
- [104] A. Guerrero-Ruiz, A. Sepulveda-Escribano, I. Rodriguez-Ramos, *Appl. Catal. A Gen.* 120 (1994) 71–83.
- [105] L.E.Y. Nonnemann, V. Ponc, *Catal. Lett.* 7 (1990) 197–203.
- [106] R. Guettel, T. Turek, *Chem. Eng. Sci.* 64 (2009) 955–964.
- [107] Y.N. Wang, Y.Y. Xu, Y.W. Li, Y.L. Zhao, B.J. Zhang, *Chem. Eng. Sci.* 58 (2003) 867–875.
- [108] C. Cao, J. Hu, S. Li, W. Wilcox, Y. Wang, *Catal. Today* 140 (2009) 149–156.
- [109] S.T. Sie, R. Krishna, *Appl. Catal. A Gen.* 186 (1999) 55–70.
- [110] R. Krishna, J.M. van Baten, M.I. Urseanu, J. Ellenberger, *Catal. Today* 66 (2001) 199–207.
- [111] Q. Hao, L. Bai, H. Xiang, Y. Li, *J. Nat. Gas Chem.* 18 (2009) 429–435.
- [112] L. Bai, H.W. Xiang, Y.W. Li, Y.Z. Han, B. Zhong, *Fuel* 81 (2002) 1577–1581.
- [113] Y.Y. Ji, H.W. Xiang, J.L. Yang, Y.Y. Xu, Y.W. Li, B. Zhong, *Appl. Catal. A Gen.* 214 (2001) 77–86.
- [114] R.L. Espinoza, A.P. Steinberg, B. Jager, A.C. Vosloo, *Appl. Catal. A Gen.* 186 (1999) 13–26.
- [115] E. van Steen, M. Claeys, *Chem. Eng. Technol.* 31 (2008) 655–666.
- [116] C.H. Zhang, Y. Yang, B.T. Teng, T.Z. Zheng, H.W. Xiang, Y.W. Li, *J. Catal.* 237 (2006) 405–415.
- [117] J.L. Casci, M.C. Lok, M.D. Shanon, *Catal. Today* 145 (2009) 38–44.
- [118] Y. Liu, B.T. Teng, X.H. Guo, *J. Mol. Catal. A Chem.* 272 (2007) 182–190.
- [119] Ø. Borg, S. Eni, E.A. Blekkan, S. Storsaeter, H. Wigum, E. Rytter, A. Holmen, *J. Catal.* 248 (2007) 89–100.
- [120] T.K. Das, G. Jacobs, P.M. Patterson, W.A. Conner, J.L. Li, B.H. Davis, *Fuel* 82 (2003) 805–815.
- [121] W. Xu, H. Li, Q. Duan, H. Ge, Xu, *Catal. Lett.* 102 (2005) 229–235.
- [122] A. Klerk, *Energy Fuel* 23 (2009) 4593–4604.
- [123] M.E. Dry, *Appl. Catal. A Gen.* 189 (1999) 185–190.
- [124] C.H. Zhang, Y. Yang, B.T. Teng, T.Z. Li, H.Y. Zheng, H.W. Xiang, Y.W. Li, *J. Catal.* 237 (2006) 405–415.
- [125] F.E.M. Farias, F.G. Sales, F.A.N. Fernandes, *J. Nat. Gas Chem.* 17 (2008) 175–178.
- [126] S. Sharifnia, Y. Mortazavi, A. Khodadadi, *Fuel Proc. Technol.* 86 (2005) 1253–1264.
- [127] S. Zheng, Y. Liu, J. Li, B. Shi, *Appl. Catal. A Gen.* 330 (2007) 63–68.
- [128] N.E. Tsakoumis, M. Ronning, O. Borg, E. Rytter, A. Holmen, *Catal. Today* 154 (2010) 162–182.
- [129] A.M. Saib, D.J. Moodley, I.M. Ciobica, M.M. Hauman, B.H. Sigwelela, C.J. Weststrate, J.W. Niemantsverdriet, J. van de Loosdrecht, *Catal. Today* 154 (2010) 271–282.
- [130] P.J. van Berge, R.C. Everson, *Stud. Surf. Sci. Catal.* 107 (1997) 207–212.
- [131] P.K. Agrawal, J.R. Katzer, W.H. Manogue, *J. Catal.* 69 (1981) 327–344.
- [132] G.C. Visconti, L. Lietti, P. Forzatti, R. Zennaro, *Appl. Catal. A Gen.* 330 (2007) 49–56.
- [133] S.C. LeVignes, C.J. Mart, W.C. Behrman, S.J. Hsia, D.R. Neskora, W.O. Patent 050487 (1998) assigned to Exxon.
- [134] E.A. Blekhan, Ø. Borg, V. Froseth, A. Holmen, *Catalysis* 20 (2007) 13–32.
- [135] J. van de Fariass, B. Balzhinimaev, J.A. Dalmon, J.W. Niemantsverdriet, S.V. Tsybulya, A.M. Saib, P.J. van Berge, J.L. Visagie, *Catal. Today* 123 (2007) 293–302.
- [136] E. van Steen, M. Claeys, M.E. Dry, J. van Loosdrecht, E.L. Viljoen, J.V. Visagie, *J. Phys. Chem. B* 109 (2005) 3575–3577.
- [137] D. Schanke, A.M. Hilmen, E. Bergene, K. Kinnari, E. Rytter, E. Adnanes, A. Holmen, *Catal. Lett.* 34 (1995) 269–284.
- [138] A.M. Hilmen, D. Schanke, K.F. Hanssen, A. Holmen, *Appl. Catal. A Gen.* 186 (1999) 169–188.
- [139] A.M. Saib, A. Borgna, J. van de Loosdrecht, P.J. van Berge, J.W. Geus, J.W. Niemantsverdriet, *J. Catal.* 239 (2006) 326–339.
- [140] A.M. Saib, A. Borgna, J. van de Loosdrecht, P.J. van Berg, J.W. Niemantsverdriet, *Appl. Catal. A Gen.* 312 (2006) 12–19.
- [141] G. Kiss, C.E. Kliewer, G.J. De Martin, C.C. Culross, J.E. Baumgartner, *J. Catal.* 217 (2003) 127–140.
- [142] G. Kiss, S. Soled, C. Kliewer, *Proceedings of the 11th International Symposium on Catalyst Deactivation Delft, The Netherlands, 2009, paper 015.*
- [143] G.L. Bezemer, J.H. Bitter, H.C.P.E. Kuipers, H. Osterbeek, J.E. Holewijn, X. Xu, F. Kapteijn, A.J. van Dillen, K.P. de Jong, *J. Am. Chem. Soc.* 128 (2006) 3956–3964.
- [144] N.O. Elbashir, P. Dutta, A. Manivannan, M.S. Seehra, C.B. Roberts, *Appl. Catal. A Gen.* 285 (2005) 169–180.
- [145] G.-Z. Bian, N. Fujishita, T. Mochizuki, W.-S. Ning, Y. Yamada, *Appl. Catal. A Gen.* 252 (2003) 251–260.

- [146] M. Ronning, N.E. Tsakoumis, A. Voronov, R.E. Johnsen, P. Norby, W. van Beek, O. Borg, E. Rytter, A. Holmen, *Catal. Today* 155 (2010) 289–295.
- [147] M.J. Overett, B. Breedt, E. du Plessis, W. Erasmus, J. van de Loosdrecht, *Prep. Pap. Am. Chem. Soc. Div. Pet. Chem.* 53 (2008) 126–128.
- [148] H. Karaca, J. Hong, P. Fongarland, P. Roussel, A. Griboval-Constant, M. Lacroix, K. Hortmann, O. Safonova, A.Y. Khodakov, *Proc. Europacat IX*, 2009, paper 011-6.
- [149] G. Jacobs, P.M. Patterson, Y. Zhang, T.K. Das, J. Li, B.H. Davis, *Appl. Catal. A Gen.* 233 (2002) 215–226.
- [150] G. Jacobs, Y. Zhang, T.K. Das, J. Li, P.M. Patterson, B.H. Davis, *Stud. Surf. Sci. Catal.* 139 (2001) 415–422.
- [151] C.H. Bartholomew, *Appl. Catal. A Gen.* 212 (2001) 17–60.
- [152] E. de Smit, B.M. Weckhuysen, *Chem. Soc. Rev.* 37 (2008) 2758–2781.
- [153] O. Ducreux, J. Lynch, B. Rebours, M. Roy, P. Chaumette, *Stud. Surf. Sci. Catal.* 119 (1998) 125–130.
- [154] P.K. Agrawal, J.R. Katzer, W.H. Manogue, *J. Catal.* 69 (1981) 312–326.
- [155] D.J. Enache, B. Rebours, M. Roy-Auberger, R. Revel, *J. Catal.* 205 (2002) 346–353.
- [156] C.H. Bartholomew, *Catal. Rev. Sci. Eng.* 24 (1982) 67–112.
- [157] M.K. Niemela, A.O.I. Krause, *Catal. Lett.* 42 (1996) 161–166.
- [158] D.J. Moodley, J. van de Loosdrecht, A.M. Saib, M.J. Overett, A.K. Datye, J. Niemantsverdriet, *Appl. Catal. A Gen.* 354 (2009) 102–110.
- [159] J. Wilson, C. de Groot, *J. Phys. Chem. B* 99 (1995) 7860–7866.
- [160] H. Schulz, *Top. Catal.* 26 (2003) 73–85.
- [161] H. Schulz, Z. Nie, F. Ousmanov, *Catal. Today* 71 (2002) 351–360.
- [162] D. Wei, J.G. Goodwin Jr., R. Oukaci, A.H. Singleton, *Appl. Catal. A Gen.* 210 (2001) 137–150.
- [163] H.H. Storch, N. Golumbic, R.B. Anderson, *The Fischer-Tropsch and Related Syntheses*, Wiley, New York, 1951.
- [164] M.E. Dry, J.R. Anderson, M. Boudart (Eds), in: *Catalysis Science and Technology*, vol. 1, Springer Verlag New-York, Heidelberg, Berlin ISBN: 0387103538. 159 pp.
- [165] R.B. Anderson, in: P.H. Emmet (Ed.), *Catalysis*, vol. 4, van Nostrand-Reinhold, New York, 1956, 257 pp.
- [166] R.B. Anderson, *The Fischer-Tropsch Synthesis* Academic Press Inc. Orlando Florida (1984).
- [167] P. Biloen, W.M.H. Sachtler, *Adv. Catal.* 30 (1981) 165.
- [168] J.P. Hindermann, G.J. Hutchings, A. Kiennemann, *Catal. Rev. Sci. Eng.* 35 (1993) 1–127.
- [169] G. Henrici-Olivé, S. Olivé, *The Chemistry of Catalyzed Hydrogenation of Carbon Monoxide*, Springer Verlag, Berlin, Heidelberg, New-York, Tokyo ISBN: 9783642696640.
- [170] V. Ponec, *Catal. Rev. Sci. Eng.* 18 (1978) 151–171.
- [171] S.R. Craxford, E.K. Rideal, *J. Chem. Soc.* (1939) 1604.
- [172] R.C. Brady, R. Pettit, *J. Am. Chem. Soc.* 102 (1980) 6182–6184.
- [173] W.A.V. van Barneveld, V. Ponec, *J. Catal.* 88 (1984) 382–387.
- [174] A.T. Bell, *Catal. Rev. Sci. Eng.* 23 (1981) 203–232.
- [175] J.T. Kummer, T.W. de Witt, P.H. Emmet, *J. Am. Chem. Soc.* 70 (1948) 3632–3643.
- [176] G. Blyholder, P.H. Emmett, *J. Phys. Chem.* 63 (1959) 962–965.
- [177] Y. Kobori, H. Yamasaki, S. Naito, T. Onishi, K. Tamaru, *J. Chem. Soc. Faraday Trans. 1* 78 (1982) 1473.
- [178] T.M. Duncan, J.A. Reimer, P. Winslow, A.T. Bell, *J. Catal.* 95 (1985) 305–308.
- [179] C.J. Wang, J.G. Ekerdt, *J. Catal.* 86 (1984) 239–244.
- [180] E.L. Muttterties, J. Stein, *Chem. Rev.* 79 (1979) 479–490.
- [181] J.T. Kummer, P.H. Emmet, *J. Am. Chem. Soc.* 75 (1953) 5177–5183.
- [182] H. Pichler, H. Schulz, *Chem. Ing. Tech.* 42 (1970) 1162–1174.
- [183] H. Schulz, A. Zein el Deen, *Fuel Proc. Technol.* 1 (1977) 45–56.
- [184] G. Henrici-Olivé, S. Olivé, *Angew. Chem. Int. Ed.* 15 (1976) 136–141.
- [185] M. Ichikawa, T. Fukushima, *J. Chem. Soc. Chem. Commun.* (1985) 321.
- [186] T.L.F. Favre, G. van der Lee, V. Ponec, *J. Chem. Soc. Chem. Commun.* (1985) 230.